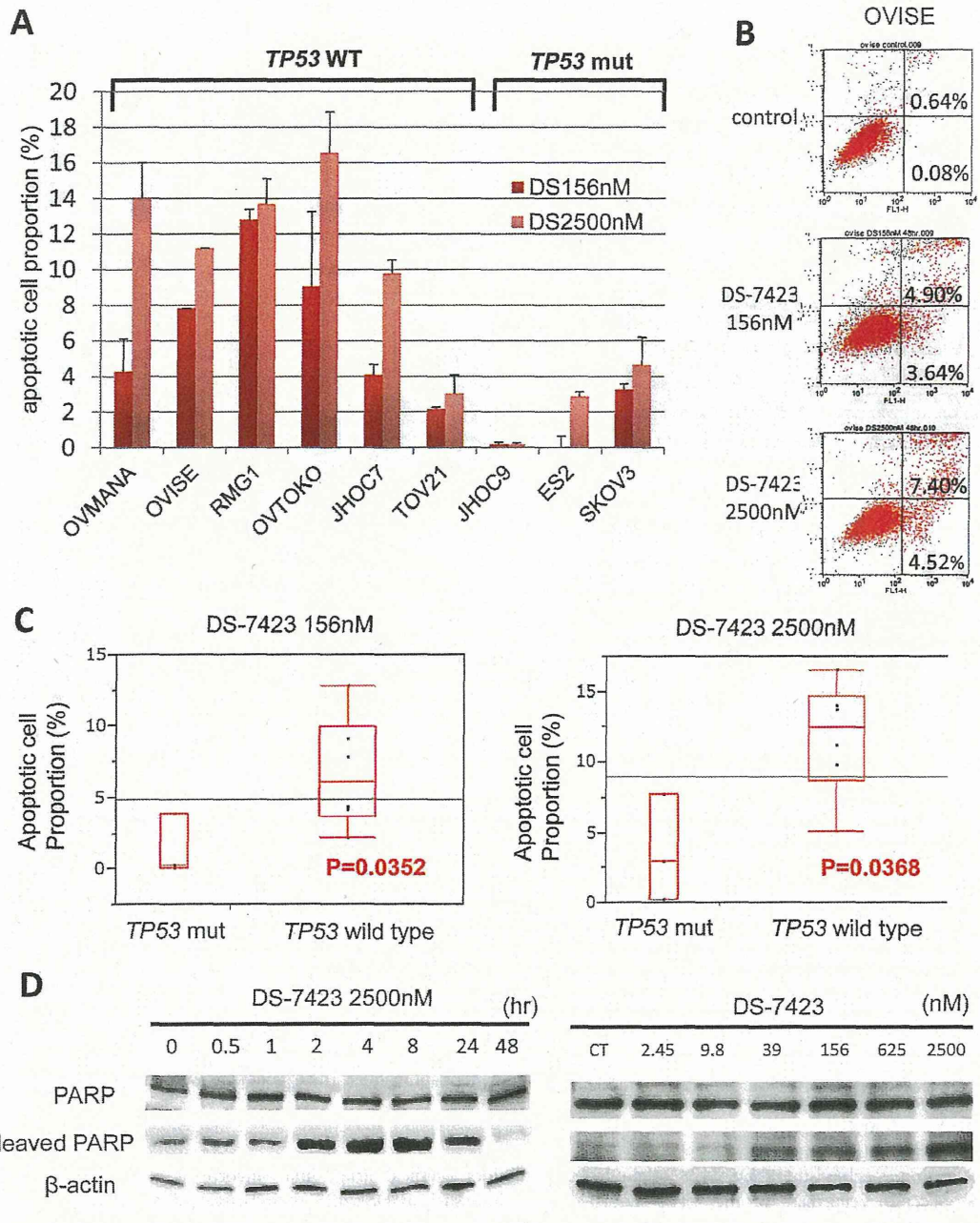

Figure 5. DS-7423–mediated induction of apoptosis in ovarian clear cell adenocarcinoma cell lines. (A) All nine OCCA cells were treated with DS-7423 at 156 or 2,560 nM for 48 h, and apoptotic cell proportion was evaluated using annexin-V fluorescein isothiocyanate (FITC) and propidium iodide (PI) double staining, followed by analysis using flow cytometry. The experiments were repeated 3 times, and each value is shown as the mean of 3 experiments ± standard deviation (SD). (B) The apoptotic cells were calculated using flow cytometry by counting the cell population in the right boxes. The example shown (OVISE cells) is representative of the results obtained for all the cell lines tested. (C) The proportion of cells rendered apoptotic by exposure to DS-7423 at 156 nM and 2,560 nM was significantly higher in OCCA cells without mutations in TP53 than in OCCA cells that carry mutations in TP53. (D) Cleaved poly(ADP-ribose) polymerase (PARP) induction was evaluated by immunoblotting in OVISE cells. OVISE cells were treated with DS-7423 at 156 nM for the times indicated (left) or for 4 h at the doses indicated (right).
doi:10.1371/journal.pone.0087220.g005

effect at the higher concentrations tested (>40 nM), rapamycin suppressed cell proliferation even at lower concentrations (<10 nM), and concentrations >10 nM failed to suppress the proliferation any further. This dose dependency is compatible with the phosphorylation levels of the target proteins in immunoblotting data and several previous reports in other types of cancers [10,12,36]. The cell cycle profile was distinct among each cell line. For example, G1 arrest was not induced and G2/M ratio was high in OVISE cells under DS-7423 exposure. This might be partly explained by the fact that GADD45 was induced by DS-7423 in

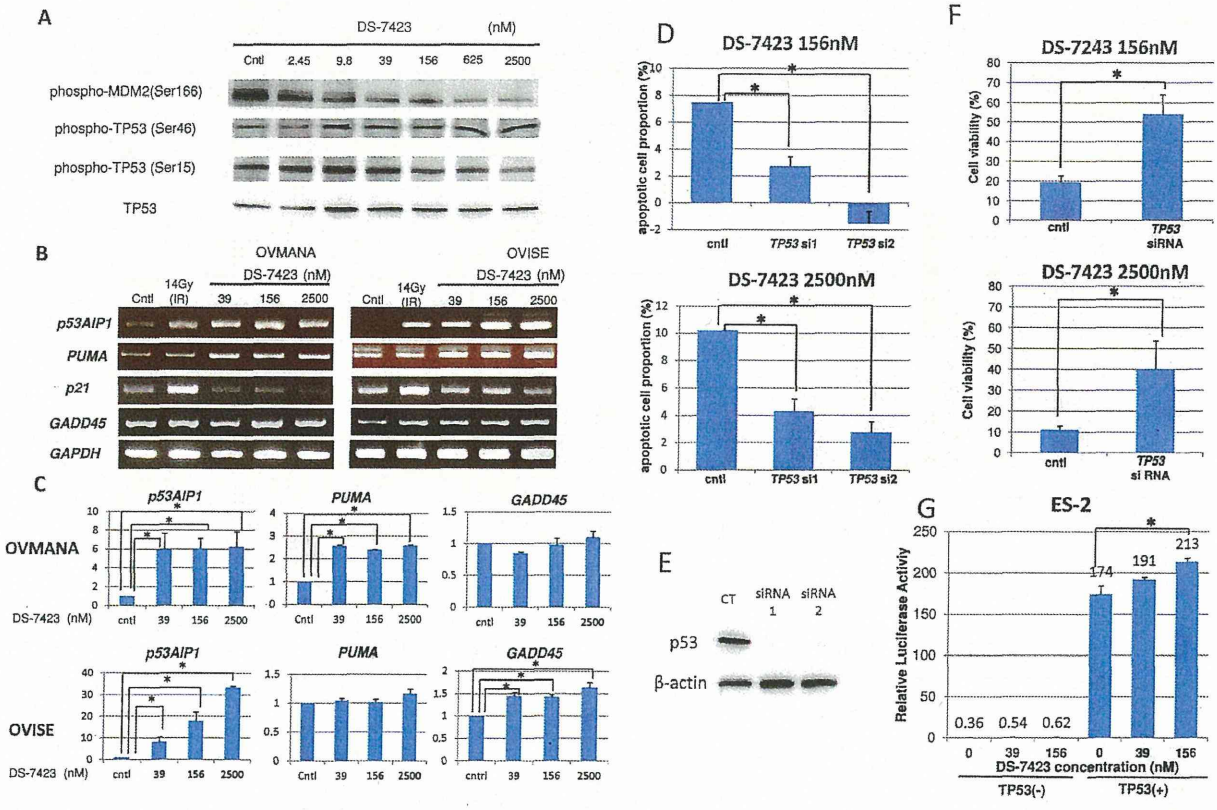

Figure 6. Induction of the phosphorylation of TP53 at Ser46 and the accumulation of transcripts of the genes targeted by TP53, which participate in TP53-mediated apoptosis. (A) Immunoblotting in OVMANA cells treated with DS-7423 at the indicated doses. Phosphorylation levels of MDM2 were inversely associated with p-TP53 at Ser46, but not with p-TP53 at Ser15. (B) Semi-quantitative RT-PCR in OVMANA and OVISE cells treated with DS-7423 at the indicated doses. Both *p53AIP1* and *PUMA* were induced by DS-7423. CT, untreated (negative) control; IR, irradiation at 14 Gy (positive control). GADD45 was induced in OVISE, but not in OVMANA cells. (C) Quantification of the semi-quantitative RT-PCR in (B). Each experiment was repeated 3 times, and each value is shown as the mean of 3 experiments ± SD. *p<0.05 (D) Effect of *TP53* knockdown on apoptosis induction by DS-7423. TP53 was knocked down by two independent siRNAs specific to *TP53* (siRNA1 and 2) in OVISE cells, which do not carry any mutation in *TP53*. The apoptotic cell population was evaluated using annexin-V staining, as described in Figure 5. The experiments were repeated 3 times, and each value is shown as the mean of 3 experiments ± SD. *p<0.05 (E) Suppression of TP53 expression by siRNAs was confirmed by immunoblotting. (F) Effect of *TP53* knockdown on cell proliferation by DS-7423 in MTT assay of OVISE cells. TP53 was knocked down by a siRNA1 specific to *TP53* and MTT assay was subsequently performed as in Figure 2. Knockdown of TP53 diminished the anti-proliferative effect caused by DS-7423 on OVISE cells. The experiments were repeated 3 times, and each value is shown as the mean of 3 experiments ± SD. *p<0.05 (G) TP53 expression plasmid (0.1 μg/μL) was cotransfected with pp53 TA Luc (0.25 μg/mL) plasmid into ES-2 cells mutated in *TP53*. The addition of DS-7423 increased the relative luciferase activity of TP53 in a dose-dependent manner. The experiments were repeated 3 times, and each value is shown as the mean of 3 experiments ± SD. *p<0.05.
doi:10.1371/journal.pone.0087220.g006

these cells. Thus, the action mechanism of DS-7423 might be distinct in each type of cells, regardless of the TP53 status. Resistance to mTOR (mTORC1) inhibitors might be induced by several mechanisms, including increased activity of another mTOR complex, mTORC2, or upregulation of receptor tyrosine kinases such as insulin-like growth factor-1 receptor (IGF-R1) [37,38]. The use of mTORC1 inhibitors to treat OCCAs is currently being investigated in phase 2 clinical trials. The currently ongoing GOG (Gynecologic Oncology Group)-0268 (NCT01196429) trial recruits OCCA patients and treats the subjects with carboplatin and paclitaxel, followed by temsirolimus (CCI-779). A report on six cases with weekly administration of temsirolimus in recurrent OCCA patients showed partial response in one patient and stable disease in another patient [39]. However, given that our data suggest that dual PI3K/mTOR inhibitors, such as DS-7423, might be more promising than single mTORC1 inhibitors, clinical trials that involve a dual PI3K/mTOR inhibitor, such as DS-7423, seem warranted for OCCA.

DS-7423 induced significantly higher levels of apoptotic cell death in OCCA cells without mutations in *TP53* than in OCCA cells with *TP53* mutations. This result suggests both that the mutational status of *TP53* might be a good biomarker to predict apoptosis induction by DS-7423, and that apoptosis depends on TP53 function. TP53 is degraded by MDM2, a ubiquitin ligase for TP53, and the MDM2 function is augmented by the kinase activity of Akt. Akt-mediated phosphorylation of MDM2 blocks its binding to p19ARF, increasing the degradation of TP53 [40,41]. DS-7423 increased the level of p-TP53 at Ser46, which results in induction of *p53AIP1* and *PUMA* (genes involved in TP53-mediated apoptosis) [29,42–44]. This data suggests that the apoptotic effect of DS-7423 depends, at least in part, on TP53 activity. The reasons for p-TP53 (Ser46), not p-TP53 (Ser15), being clearly induced and for apoptosis being preferentially

induced by high doses of DS-7423 should be further clarified. In addition, other non-apoptotic genes were not significantly induced by DS-7423, except for GADD45 in OVISE cells. Further analyses are warranted whether TP53 function is more involved in apoptosis rather than in cell cycle arrest and/or DNA repair process by DS-7423. Another possibility is that other proteins (such as FOXOs) which act downstream of Akt might also play a role in the induction [45]. Dephosphorylation of FOXOs at their Akt sites induces their nuclear translocation and triggers apoptosis by induction of prosurvival genes of the BCL2 family [46,47]. The observation that the phosphorylation of FOXO1/3a was suppressed by DS-7423, regardless of TP53 status, suggests that the pro-apoptotic effect of DS-7423 cannot be explained exclusively by the phosphorylation of FOXOs. The use of siRNA to knockdown TP53 rescued OCCA cells from apoptosis caused by DS-7423. We also confirmed by MTT assay that the anti-proliferative effect of DS-7423 was significantly diminished by knocking down TP53, suggesting that intact TP53 function might enhance the anti-tumor effect of DS-7423. Recently, it was reported that cell death caused by a PI3K inhibitor, BKM-120, was associated with TP53 status in glioma cells [48], and that PI3K/AKT inhibition was suggested to induce TP53-dependent apoptosis in HTLV-1-transformed cells [49]. These data also support the importance of wild-type TP53 in the induction of the cytotoxic effect of PI3K pathway inhibitors.

The involvement of multiple molecules in the activation of the PI3K/mTOR pathway underscores the critical need to develop predictive biomarkers that might also serve as therapeutic targets. Mutations of *PIK3CA* and amplification of *HER2* have been proposed to be useful biomarkers in breast cancer [50,51], whereas mutant Ras has been suggested to be a biomarker of resistance in several solid tumor cells [52]. All these biomarkers (*PIK3CA*, HER2 and Ras) are focused on the RTK/Ras/PI3K pathway itself, and not on the cytotoxic effects associated with PI3K/mTOR inhibitors. Our data suggest that the presence of *PIK3CA* mutation and any other PI3K-activating alteration alone might not predict the sensitivity of OCCA cells to DS-7423. ES-2 cells, with no mutations in the RTK/Ras/PI3K pathway genes examined, showed low level of p-Akt, and the effect of DS-7423 in ES-2 xenografts was less robust, suggesting that the level of PI3K pathway activation would still be important for the sensitivity. However, the mutational status of TP53 might represent a better biomarker for the selection of tumors that could be killed by DS-7423 treatment. The frequency of mutations in *TP53* in OCCA was much less frequent than for ovarian cancers with other histology types [15,53]. These results indicate that OCCAs would be good candidates for clinical studies on the dual PI3K/mTOR inhibitor, DS-7423.

Our study has several limitations. First, cytostatic effect is still essential to suppress cell proliferation, regardless of TP53 status. Second, the ratio of apoptotic cells is low (less than 20%) even at high concentrations of DS-7423. Third, the mechanism of cytostatic effect by DS-7423 in OCCA is cell type dependent (i.e. G1 arrest was not induced in OVISE and ES-2 cells). Thus, careful consideration is required to evaluate the TP53-dependent cytotoxic effect of DS-7423. Further studies are warranted to elucidate the mechanism of action of DS-7423, and more efficient induction of apoptosis might be needed for clinical application of this drug in OCCA.

Supporting Information

Figure S1 Immunoblotting of OCCA cells (ES-2 and JHOC-9), treated with DS-7423 at concentrations ranging from 0 to 2,500 nmol/L. As shown in Figure 3, phosphorylation of AKT and its target proteins were downregulated by DS-7423. In ES-2 cells, basal level of p-AKT at Thr 308 was very low (as shown in Fig. 1), but p-AKT at Ser473 was clearly suppressed by DS-7423.
(PPTX)

Figure S2 *In vivo* effect of DS-7423 in nude mice. (A) Western blot of total lysates from the TOV-21G and RMG-1 xenografts. total lysates were harvested 2 and 6 h after the last drug administration of DS-7423. The levels of p-Akt (Thr-308) and p-S6 (Ser-240/244) were assessed. (B) Subcutaneous xenograft tumors in athymic BALB/c mice were established after injection of ES-2 cells. Mice were treated daily at the indicated doses (1.5, 3 or 6 mg/kg/day, totally 8 times) of DS-7423 or non-treated control. Estimated tumor volumes were smaller in mice treated daily with 6 mg/kg of DS-7423, compared to the control. Western blot of total lysates from the ES-2 xenografts (treated with 6 mg/kg of DS-7423) was also shown below.
(PPTX)

Figure S3 The size of apoptotic cell population was compared between DS-7423 and rapamycin in OVISE cells, using annexin-V FITC and PI double staining (as shown in Fig. 5A–5B). The percentage of apoptotic cells was significantly higher in cells treated with DS-7423, compared with those with rapamycin.
(PPTX)

Figure S4 Semi-quantitative RT-PCR in OVMANA and OVISE cells treated with DS-7423 at the indicated doses. Each expression level of p53R2, TIGAR, GLS2, GADD45, 14-3-3 sigma and PAI-1 was not enhanced by DS-7423. Each experiment was repeated 3 times, and each value is shown as the mean of 3 experiments ± SD.
(PPTX)

Table S1 Phosphorylation and mutational status in 9 OCCA cell lines. Elevated phosphorylation of cMET, HER2 and HER3, and mutations of *PIK3CA*, *PTEN*, *KRAS* and *TP53* were listed in each cell line.
(XLSX)

Acknowledgments

We thank Satoru Kyo for the generous gift of the immortalized cell line.

Author Contributions

Conceived and designed the experiments: T Kashiyama KO YS YH KM. Performed the experiments: T Kashiyama YI YS YH KI CM RK. Analyzed the data: T Kashiyama KO YS YH. Contributed reagents/materials/analysis tools: YI AM T Koso T Fukuda MT K Shoji K Sone TA OW-H KK SN KM FM HA TY YO T Fujii. Wrote the paper: T Kashiyama KO.

References

1. Yuan TL, Cantley LC (2008) PI3K pathway alterations in cancer: variations on a theme. Oncogene 27: 5497–510.
2. Jia S, Liu Z, Zhang S, Liu P, Zhang L, et al. (2008) Essential roles of PI(3)K-p110beta in cell growth, metabolism and tumorigenesis. Nature 454: 776–9.
3. Wee S, Wiederschain D, Maira SM, Loo A, Miller C, et al. (2008) PTEN-deficient cancers depend on PIK3CB. Proc Natl Acad Sci USA 105: 13057–13062.
4. Zoncu R, Efeyan A, Sabatini DM (2011) mTOR: from growth signal integration to cancer, diabetes and ageing. Nat Rev Mol Cell Biol 12: 21–35.

5. Engelman JA (2009) Targeting PI3K signalling in cancer: opportunities, challenges and limitations. Nat Rev Cancer 9: 550–562.
6. Sabatini DM (2006) mTOR and cancer: insights into a complex relationship. Nat Rev Cancer 6: 729–734.
7. Guertin DA, Sabatini DM (2007) Defining the role of mTOR in cancer. Cancer Cell 12: 9–22.
8. Mayo LD, Donner DB (2001) A phosphatidylinositol 3-kinase/Akt pathway promotes translocation of Mdm2 from the cytoplasm to the nucleus. Proc Natl Acad Sci USA 98: 11598–11603.
9. Maira SM, Stauffer F, Brueggen J, Furet P, Schnell C, et al. (2008) Identification and characterization of NVP-BEZ235, a new orally available dual phosphatidylinositol 3-kinase/mammalian target of rapamycin inhibitor with potent in vivo antitumor activity. Mol Cancer Ther 7: 1851–1863.
10. Serra V, Markman B, Scaltriti M, Eichhorn PJ, Valero V, et al. (2008) NVP-BEZ235, a dual PI3K/mTOR inhibitor, prevents PI3K signaling and inhibits the growth of cancer cells with activating PI3K mutations. Cancer Res 68: 8022–8030.
11. Cao P, Maira SM, Garcia Echeverria C, Hedley DW (2009) Activity of a novel, dual PI3-kinase/mTor inhibitor NVP-BEZ235 against primary human pancreatic cancers grown as orthotopic xenografts. Br J Cancer 100: 1267–1276.
12. Shoji K, Oda K, Kashiyama T, Ikeda Y, Nakagawa S, et al. (2012) Genotype-dependent efficacy of a dual PI3K/mTOR inhibitor, NVP-BEZ235, and an mTOR inhibitor, RAD001, in endometrial carcinomas. PLoS One 7: e37431.
13. Anglesio MS, Carey MS, Kobel M, Mackay H, Huntsman DG (2011) Clear cell carcinoma of the ovary: A report from the first Ovarian Clear Cell Symposium, June 24th, Gynecol Oncol 2010. 121: 407–415.
14. Takano M, Tsuda H, Sugiyama T (2012) Clear cell carcinoma of the ovary: is there a role of histology-specific treatment? J Exp Clin Cancer Res 31: 53–59.
15. Bell D, Berchuck A, Birrer M, Chien J, Cramer D, et al. (2011) Integrated genomic analyses of ovarian carcinoma. Nature 474: 609–615. Cancer Genome Atlas Research Network.
16. Ho ES, Lai CR, Hsieh YT, Chen JT, Lin AJ, et al. (2001) p53 mutation is infrequent in clear cell carcinoma of the ovary. Gynecol Oncol 80: 189–193.
17. Kuo KT, Mao TL, Jones S, Veras E, Ayhan A, et al. (2009) Frequent activating mutations of PIK3CA in ovarian clear cell carcinoma. Am J Pathol 174: 1597–1601.
18. Munksgaard PS, Blaakaer J (2012) The association between endometriosis and ovarian cancer: a review of histological, genetic and molecular alterations. Gynecol Oncol 124: 164–169.
19. Fujimura M, Katsumata N, Tsuda H, Uchi N, Miyazaki S, et al. (2002) HER2 is frequently over-expressed in ovarian clear cell adenocarcinoma: possible novel treatment modality using recombinant monoclonal antibody against HER2, trastuzumab. Jpn J Cancer Res 93: 1250–1257.
20. Yamamoto S, Tsuda H, Miyai K, Takano M, Tamai S, et al. (2011) Gene amplification and protein overexpression of MET are common events in ovarian clear-cell adenocarcinoma: their roles in tumor progression and prognostication of the patient. Mod Pathol 24: 1146–1155.
21. Yamamoto S, Tsuda H, Miyai K, Takano M, Tamai S, et al. (2012) Accumulative copy number increase of MET drives tumor development and histological progression in a subset of ovarian clear-cell adenocarcinomas. Mod Pathol 25: 122–130.
22. Shaw TJ, Senterman MK, Dawson K, Crane CA, Vanderhyden BC (2004) Characterization of intraperitoneal, orthotopic, and metastatic xenograft models of human ovarian cancer. Mol Ther 10: 1032–1042.
23. Bono Y, Kyo S, Takakura M, Maida Y, Mizumoto Y, et al. (2012) Creation of immortalised epithelial cells from ovarian endometrioma. Br J Cancer 106: 1205–1213.
24. Minaguchi T, Yoshikawa H, Oda K, Ishino T, Yasugi T, et al. (2001) PTEN mutation located only outside exons 5, 6, and 7 is an independent predictor of favorable survival in endometrial carcinomas. Clin Cancer Res 7: 2636–2642.
25. Samuels Y, Wang Z, Bardelli A, Silliman N, Ptak J, et al. (2004) High frequency of mutations of the PIK3CA gene in human cancers. Science 304: 554.
26. Oda K, Stokoe D, Taketani Y, McCormick F (2005) High frequency of coexistent mutations of PIK3CA and PTEN genes in endometrial carcinoma. Cancer Res 65: 10669–10673.
27. Oda K, Okada J, Timmerman L, Rodriguez Viciana P, Stokoe D, et al. (2008) PIK3CA cooperates with other phosphatidylinositol 3′-kinase pathway mutations to effect oncogenic transformation. Cancer Res 68: 8127–8136.
28. Nakagawa S, Yoshikawa H, Jimbo H, Onda T, Yasugi T, et al. (1999) Elderly Japanese women with cervical carcinoma show higher proportions of both intermediate-risk human papillomavirus types and p53 mutations. Br J Cancer 79: 1139–1144.
29. Oda K, Arakawa H, Tanaka T, Matsuda K, Tanikawa C, et al. (2000) p53AIP1, a potential mediator of p53-dependent apoptosis, and its regulation by Ser-46-phosphorylated p53. Cell 102: 849–862.
30. Hermeking H, Lengauer C, Polyak K, He TC, Zhang L, et al (1997) 14-3-3 sigma is a p53-regulated inhibitor of G2/M progression. Mol Cell 1: 3–11.
31. Zhan Q, Antinore MJ, Wang XW, Carrier F, Smith ML, et al (1999) Association with Cdc2 and inhibition of Cdc2/Cyclin B1 kinase activity by the p53-regulated protein Gadd45. Oncogene 18: 2892–2900.
32. Tanaka H, Arakawa H, Yamaguchi T, Shiraishi K, Fukuda S, et al (2000) A ribonucleotide reductase gene involved in a p53-dependent cell-cycle checkpoint for DNA damage. Nature 404: 42–49.
33. Kortlever RM, Higgins PJ, Bernards R (2006) Plasminogen activator inhibitor-1 is a critical downstream target of p53 in the induction of replicative senescence. Nat Cell Biol 8: 877–884.
34. Bensaad K, Tsuruta A, Selak MA, Vidal MN, Nakano K, et al (2006) TIGAR, a p53-inducible regulator of glycolysis and apoptosis. Cell 126: 107–120.
35. Suzuki S, Tanaka T, Poyurovsky MV, Nagano H, Mayama T, et al (2010) Phosphate-activated glutaminase (GLS2), a p53-inducible regulator of glutamine metabolism and reactive oxygen species. Proc Natl Acad Sci U S A 107: 7461–7466.
36. Cho DC, Cohen MB, Panka DJ, Collins M, Ghebremichael M, et al. (2010) The efficacy of the novel dual PI3-kinase/mTOR inhibitor NVP-BEZ235 compared with rapamycin in renal cell carcinoma. Clin Cancer Res 16: 3628–3638.
37. O'Reilly KE, Rojo F, She QB, Solit D, Mills GB, et al. (2006) mTOR inhibition induces upstream receptor tyrosine kinase signaling and activates Akt. Cancer Res 66: 1500–1508.
38. Wan X, Harkavy B, Shen N, Grohar P, Helman LJ (2007) Rapamycin induces feedback activation of Akt signaling through an IGF-1R-dependent mechanism. Oncogene 26: 1932–1940.
39. Takano M, Kikuchi Y, Kudoh K, Goto T, Furuya K, et al. (2011) Weekly administration of temsirolimus for heavily pretreated patients with clear cell carcinoma of the ovary: a report of six cases. Int J Clin Oncol 16: 605–609.
40. Haupt Y, Maya R, Kazaz A, Oren M (1997) Mdm2 promotes the rapid degradation of p53. Nature 387: 296–299.
41. Ogawara Y, Kishishita S, Obata T, Isazawa Y, Suzuki T, et al. (2002) Akt enhances Mdm2-mediated ubiquitination and degradation of p53. J Biol Chem 277: 21843–21850.
42. Nakano K, Vousden KH (2001) PUMA, a novel proapoptotic gene, is induced by p53. Mol Cell 7: 683–694.
43. Matsuda K, Yoshida K, Taya Y, Nakamura K, Nakamura Y, et al. (2002) p53AIP1 regulates the mitochondrial apoptotic pathway. Cancer Res 62: 2883–2889.
44. Vousden KH, Prives C (2009) Blinded by the Light: The Growing Complexity of p53. Cell 137: 413–421.
45. Fu Z, Tindall DJ (2008) FOXOs, cancer and regulation of apoptosis. Oncogene 27: 2312–2319.
46. Rahmani M, Anderson A, Habibi JR, Crabtree TR, Mayo M, et al. (2009) The BH3-only protein Bim plays a critical role in leukemia cell death triggered by concomitant inhibition of the PI3K/Akt and MEK/ERK1/2 pathways. Blood 114: 4507–4516.
47. Letai A (2006) Growth factor withdrawal and apoptosis: the middle game. Mol Cell 21: 728–730.
48. Koul D, Fu J, Shen R, LaFortune TA, Wang S, et al (2012) Antitumor activity of NVP-BKM120– a selective pan class I PI3 kinase inhibitor showed differential forms of cell death based on p53 status of glioma cells. Clin Cancer Res 18: 184–195.
49. Jeong SJ, Dasgupta A, Jung KJ, Um JH, Burke A, et al (2008) PI3K/AKT inhibition induces caspase-dependent apoptosis in HTLV-1-transformed cells. Virology 370: 264–272.
50. She QB, Chandarlapaty S, Ye Q, Lobo J, Haskell KM, et al. (2008) Breast tumor cells with PI3K mutation or HER2 amplification are selectively addicted to Akt signaling. PLoS One 3: e3065.
51. O'Brien C, Wallin JJ, Sampath D, GuhaThakurta D, Savage H, et al. (2010) Predictive biomarkers of sensitivity to the phosphatidylinositol 3′ kinase inhibitor GDC-0941 in breast cancer preclinical models. Clin Cancer Res 16: 3670–3683.
52. Ihle NT, Lemos R Jr, Wipf P, Yacoub A, Mitchell C, et al. (2009) Mutations in the phosphatidylinositol-3-kinase pathway predict for antitumor activity of the inhibitor PX-866 whereas oncogenic Ras is a dominant predictor for resistance. Cancer Res 69: 143–150.
53. Petitjean A, Achatz MI, Borresen Dale AL, Hainaut P, et al. (2005) TP53 mutations in human cancers: functional selection and impact on cancer prognosis and outcomes. Oncogene 26: 2157–2165.

OPEN ACCESS Freely available online

PLOS ONE

Matrix Metalloproteinase (MMP)-9 in Cancer-Associated Fibroblasts (CAFs) Is Suppressed by Omega-3 Polyunsaturated Fatty Acids *In Vitro* and *In Vivo*

Ayumi Taguchi[1], Kei Kawana[1*☯], Kensuke Tomio[1], Aki Yamashita[1], Yosuke Isobe[2], Kazunori Nagasaka[1], Kaori Koga[1], Tomoko Inoue[1], Haruka Nishida[1], Satoko Kojima[1], Katsuyuki Adachi[1], Yoko Matsumoto[1], Takahide Arimoto[1], Osamu Wada-Hiraike[1], Katsutoshi Oda[1], Jing X. Kang[3], Hiroyuki Arai[2], Makoto Arita[2*☯], Yutaka Osuga[1], Tomoyuki Fujii[1]

1 Department of Obstetrics and Gynecology, Graduate School of Medicine, The University of Tokyo, 7-3-1 Hongo, Bunkyo-ku, Tokyo, Japan, **2** Department of Health Chemistry, Graduate School of Pharmaceutical Sciences, The University of Tokyo, 7-3-1 Hongo, Bunkyo-ku, Tokyo, Japan, **3** Department of Medicine, Massachusetts General Hospital and Harvard Medical School, Charlestown, Massachusetts, United States of America

Abstract

Cancer associated fibroblasts (CAFs) are responsible for tumor growth, angiogenesis, invasion, and metastasis. Matrix metalloproteinase (MMP)-9 secreted from cancer stroma populated by CAFs is a prerequisite for cancer angiogenesis and metastasis. Omega-3 polyunsaturated fatty acids (omega-3 PUFA) have been reported to have anti-tumor effects on diverse types of malignancies. Fat-1 mice, which can convert omega-6 to omega-3 PUFA independent of diet, are useful to investigate the functions of endogenous omega-3 PUFA. To examine the effect of omega-3 PUFA on tumorigenesis, TC-1 cells, a murine epithelial cell line immortalized by human papillomavirus (HPV) oncogenes, were injected subcutaneously into fat-1 or wild type mice. Tumor growth and angiogenesis of the TC-1 tumor were significantly suppressed in fat-1 compared to wild type mice. cDNA microarray of the tumors derived from fat-1 and wild type mice revealed that MMP-9 is downregulated in fat-1 mice. Immunohistochemical study demonstrated immunoreactivity for MMP-9 in the tumor stromal fibroblasts was diffusely positive in wild type whereas focal in fat-1 mice. MMP-9 was expressed in primary cultured fibroblasts isolated from fat-1 and wild type mice but was not expressed in TC-1 cells. Co-culture of fibroblasts with TC-1 cells enhanced the expression and the proteinase activity of MMP-9, although the protease activity of MMP-9 in fat-1-derived fibroblasts was lower than that in wild type fibroblasts. Our data suggests that omega-3 PUFAs suppress MMP-9 induction and tumor angiogenesis. These findings may provide insight into mechanisms by which omega-3 PUFAs exert anti-tumor effects by modulating tumor microenvironment.

Citation: Taguchi A, Kawana K, Tomio K, Yamashita A, Isobe Y, et al. (2014) Matrix Metalloproteinase (MMP)-9 in Cancer-Associated Fibroblasts (CAFs) Is Suppressed by Omega-3 Polyunsaturated Fatty Acids *In Vitro* and *In Vivo*. PLoS ONE 9(2): e89605. doi:10.1371/journal.pone.0089605

Editor: Zhongjun Zhou, The University of Hong Kong, Hong Kong

Received October 10, 2013; **Accepted** January 22, 2014; **Published** February 27, 2014

Funding: This study was funded by Tokyo IGAKUKAI (K.K.), the Japan Science and Technology Agency Precursory Research for Embryonic Science and Technology (PRESTO) (M.A.), the Ministry of Education, Culture, Sports, Science, and Technology of Japan (M.A.). The funders had no role in study design, data collection and analysis, decision to publish, or preparation of the manuscript.

Competing Interests: The authors have declared that no competing interests exist.

* E-mail: kkawana-tky@umin.org (K. Kawana); marita@mol.f.u-tokyo.ac.jp (MA)

☯ These authors contributed equally to this work.

Introduction

The tumor microenvironment is comprised of microvascular endothelial cells, adjacent normal epithelial cells and cancer-associated fibroblasts (CAFs), and is reported to be an important regulator of tumorigenesis [1,2]. As the most common cellular population found in the tumor microenvironment, CAFs are responsible for the synthesis of proteins involved in the remodeling of the extracellular matrix (ECM), and for the secretion of growth factors and cytokines that regulate tumor cell proliferation and invasion [3,4]. In murine ovarian cancer xenograft models, the p53/NF-κB pathway in CAFs significantly increased in vivo tumor growth [5]. In colon cancer, Zhu Y et al. report that IL-1β increased colon cancer cell proliferation and invasion by up-regulating COX-2 signaling in CAFs [6].

Matrix-metalloproteinases (MMPs) are synthesized as proenzymes and typically activated by proteolytic removal of a propeptide [7]. MMPs are reported to influence tumor progression by facilitating events pivotal for neovascularization and establishment of distant metastasis including proliferation, survival and migration of endothelial, tumor and stromal cells [8,9]. MMP-2 and MMP-9 are implicated as prerequisites for angiogenesis and metastasis in the carcinogenesic process. MMP-2 is expressed in the various cancer cell lines [10]. In contrast, MMP-9 has very limited or no expression in these cancer cells. Instead, MMP-9 is well-known to be secreted from cancer stromal fibroblasts and endothelial cells [11,12]. MMP-9 is a member of a family of zinc containing endoproteinases that is involved in degradation of extracellular matrix (ECM) and in vascular remodeling [13].

Docosahexaenoic acid (DHA, 22:6n-3) and eicosapentaenoic acid (EPA, 20:5n-3) are representative mediators of omega-3

polyunsaturated fatty acids (omega-3 PUFAs) and exert anti-inflammatory effects in acute and chronic pathological inflammatory reactions by counteracting inflammation [14]. Omega-3 PUFAs are also reported to have anti-cancer effects based on in vitro and vivo studies [15–17]. Several mechanisms have been proposed to explain the anti-cancer effects of omega-3 PUFAs. Omega-3 PUFAs alter the growth of tumor cells by modulating cell replication, by interfering with components of the cell cycle or by increasing cell death via necrosis or apoptosis [18,19]. Omega-3 PUFAs are also known to exert anti-angiogenic effects by inhibiting the production of many angiogenic mediators including: vascular endothelial growth factor (VEGF), platelet-derived growth factor (PDGF), and prostaglandin E2 (PGE2) [20–24].

Dietary supplementation is a traditional approach to modify tissue nutrient composition in animal studies of nutrition. Feeding animals diets that alter specific nutritional and non-nutritional components can help to differentiate experimental groups; however, it can be exceedingly difficult to provide diets that are identical in all but a single or a small but controlled number of components. Kang et al. recently engineered a transgenic mouse that carries the fat-1 gene from the roundworm *Caenorhabditis elegans* [25]. This gene encodes an omega-3 fatty acid desaturase that catalyzes the conversion of omega-6 to omega-3 PUFAs and that is absent in most animals, including mammals. There is a remarkable difference in the tissue omega-6/omega-3 PUFA ratio between wild type and fat-1 transgenic mice [26]. Fat-1 mice, which typically exhibit a balanced ratio of omega-6 to omega-3 PUFAs in their tissues and organs independent of diet, allow carefully controlled studies to be performed in the absence of potential confounding factors of diet. This makes them a useful model to investigate the biological properties of endogenous omega-3 PUFAs [25]. Several reports using fat-1 mice have demonstrated anti-cancer effects of omega-3 PUFAs [27–30]. In these investigations, omega-3 PUFAs exerted anti-cancer effects by suppressing inflammatory reactions and PGE2 secretion from cancer cells. To date, there are few studies that investigate the involvement of omega-3 PUFAs in the biology of CAFs.

In this study, we hypothesized that omega-3 PUFAs may alter tumor microenvironments by influencing CAF activity. To examine this hypothesis, fibroblasts derived from fat-1 and wild type mice were assessed both in vitro and in vivo under conditions allowing interaction with TC-1 cancer cells. TC-1 cells were derived from the epithelium of C56BL/6 mice and immortalized by human papillomavirus (HPV) type 16 E6 and E7 oncoproteins. They are commonly used in vitro and in vivo in murine models of HPV-related cancer [31]. Here, we investigated the involvement of omega-3 PUFAs in TC-1 tumorigenesis by comparing fat-1 and wild type mice. Our specific focus involved the study of tumor-associated fibroblasts. These models are useful in the study of CAFs because the cancer cells originate in wild type murine epithelium while the cancer stromal components, including CAFs, come from fat-1 (omega-3 PUFAs-rich) or wild type (normal PUFAs) mice.

Materials and Methods

Animals and diet

Fat-1 mice were created on a C57BL/6 background as described [26] and subsequently backcrossed (at least four times) onto a C57BL/6 background. Animals were fed a special diet (AIN-76A+10% safflower oil; CLEA Japan, Inc.) that contained 10.3% total fat with fatty acid composition of C16:0 (7.6%), C18:0 (2.7%), C18:1n-9 (14.1%), C18:2n-6 (73.2%), C18: 3n-3 (0.3%), C20:4n-6 (<0.1%), C20:5n-3 (<0.1%), C22: 6n-3 (<0.1%), high in n-6 and low in n-3 fatty acids, until the desired age (6–8 weeks) for experiments. To prevent the oxidation of lipids in the diet, all foods were stored in the refrigerator with antioxidants (AGELESS; Mitsubishi Gas Chemical Inc.), and prepared newly every two days. Animal studies were approved by the University of Tokyo Animal Committee.

Tumor growth assay in mice

TC-1 cells are derived from a primary lung epithelial cell from C56BL6/mice and immortalized using HPV 16 E6/E7 plus c-Has-ras (kind gift from Dr. T. C. Wu, Johns-Hopkins University, Baltimore MD USA) [32]. TC-1 cells were cultured in DMEM (Gibco, NY, USA) containing 10% FBS, 100 U/ml penicillin, 0.1 mg/ml streptomycin, and 0.25 g/ml amphotericin B. Eight-week-old female mice were injected with 5×10^6 murine TC-1 cells suspended in 100 µl of DMEM. Tumor volume, based on caliper measurements, was calculated at 7 and 14 days after injection according to the following formula: (tumor volume) = $1/2\times$(the shortest diameter) $^2\times$(the largest diameter). Mice were sacrificed 14 days after inoculation, tumors were excised and stored at −80°C for future analyses.

cDNA microarray

Total RNA from TC-1 tumors (above) was extracted using an RNeasy minikit (QIAGEN, Hilden, Germany). For the cDNA microarray analysis, 0.5 µg of pooled total RNA was amplified and labeled using an Amino Allyl MessageAmpTM II mRNA Amplification kit (Applied Biosystems, Foster City, CA, USA) according to the manufacturer's instructions. Each sample of mRNA labeled with Cy3 and reference mRNA labeled with Cy5 was cohybridized to the GeneTM Mouse Oligo chip 24 k (Toray Industries Inc., Tokyo, Japan) at 37°C for 16 h. After hybridization, each DNA chip was washed and dried. Hybridization signals derived from Cy3 and Cy5 were scanned using Scan Array Express (PerkinElmer, Waltham, MA, USA). The scanned image was analyzed using GenePix Pro (MDS Analytical Technologies, Sunnyvale, CA, USA). All analyzed data were scaled by global normalization. GEO accession number is GSE54079.

Immunohistochemistry

Paraffin sections (4 µm) of TC-1 tumors were dewaxed in xylene and rehydrated through graded ethanol to water. Antigens were retrieved by boiling in 10 mM citrate buffer (pH 6.0) for 30 min. The cooled sections were incubated in DAKO REAL Peroxidase-Blocking solution (DAKO, Carpinteria, CA, USA) for 10 min to quench endogenous peroxidase. To block nonspecific binding, sections were incubated in DAKO Protein Blocking solution (DAKO) for 10 min at room temperature. Sections were then incubated with a rabbit polyclonal antibody against mouse MMP-9 (PAB12714, Abnova, 1:100 dilution) in DAKO REAL Antibody Diluent (DAKO) overnight at 4°C. The slides were incubated for 1 hour at room temperature with peroxidase-conjugated secondary antibodies, washed, incubated with DAB, counterstained with hematoxylin, dehydrated through an ethanol series and xylene, and mounted. To evaluate tumor microvessel formation, tumor sections were stained for CD-31 using a rat monoclonal antibody against mouse CD-31 (ab56299, Abcam, Tokyo, Japan, 1:100 dilution).

RT-quantitative PCR (RT-qPCR)

Total RNA was extracted from TC-1 tumors and cultured fibroblasts using an RNeasy minikit (QIAGEN, Hilden, Germany), followed by reverse transcription. cDNA was amplified for

40 cycles in a Light Cycler 480 (Roche, Basel, Switzerland) using a Universal Probe Master Mix and the following primers and Universal Probe Library (UPL) probes (Roche). The primer pairs and the universal probes corresponding to the each primer that were used in amplifications were as follows: mouse β-actin, 5′-ATTGAAACATCAGCCAAGACC-3′ and 5′-CCGAATCTCA-CGGACTAGTGT-3′ probe88; mouse MMP-9, 5′-ACGACA-TAGACGGCATCCA-3′ and 5′-GCTGTGGTTCAGTTGTG-GTG-3′ probe19. Expression of MMP-9 was normalized using β-actin mRNA as an internal standard. Expression levels were calculated by the comparative Ct method using β-actin as an endogenous reference gene.

Primary fibroblast culture and co-culture with TC-1 cells

Lungs were isolated from fat-1 transgenic and wild type mice and washed with saline to remove blood cells. Isolation and culture of pulmonary fibroblasts were performed using methods described previously [33]. Lung tissues were minced into small pieces and incubated in DMEM (Gibco, NY, USA) containing type I collagenase (0.25%; Sigma-Aldrich, St Louis, MO, USA) and deoxynuclease I (15 U/ml; TaKaRa, Tokyo, Japan) for 120 min at 37°C. The resultant dispersed cells were separated by filtration through nylon cell strainers (70 μm, BD, Franklin Lakes, NJ, USA). Fibroblasts in the filtrate were collected, placed into 10 cm dishes in DMEM containing 10% FBS, 100 U/ml penicillin, 0.1 mg/ml streptomycin, and 0.25 mg/l amphotericin B, and incubated for 7–10 days. Fibroblasts were purified from other cell population by differential adhesion and serial passage.

Confluent fibroblasts and TC-1 cells were trypsinized and resuspended in DMEM containing 10% FBS, 100 U/ml penicillin, 0.1 mg/ml streptomycin, and 0.25 g/ml amphotericin B and 1×10^5 cells/ml cells of each cell type were plated together in 12 well culture plates. Co-cultures were incubated at 37°C 5% CO2 in a humidified atmosphere for 24 hours. Homotypic cultures served as controls.

Gelatin zymography

Gelatin zymography assays were performed using a Gelatin zymography kit (Cosmobio, Sapporo, Japan) according to the manufacture's instuctions. Cell culture supernatants were collected and centrifuged at 1,500 rpm for 5 minutes. The cell free supernatant was mixed with 2× sample buffer and electrophoresed using precast gels (10% polyacrylamide, 0.1% gelatin) at 4°C for 1 hour. Subsequentnzymatic reactions were performed at 37°C overnight. Gelatinase activities were visualized using specific staining solutions and destained in acetic acid-methanol-dH_2O (1:3:6). For semi-quantitative analyses, gelatin zymography bands were analyzed using image analysis software (ImageJ).

Statistical analysis

Data are presented as means ± SEM. Statistical analyses were carried out by Student's *t*-test, or Wilcoxon analysis using JMP software. A value of $P<0.05$ was considered significant. In the figure legends, asterisks indicate those comparisons with statistical significance ($p<0.05$).

Results

Tumor growth and angiogenesis of TC-1 tumors is suppressed in fat-1 mice

To investigate the effect of omega-3 PUFAs on cervical cancer tumorigenesis, we injected TC-1 cells subcutaneously into fat-1 and the litter-mate wild type C57/BL6 mice. TC-1 tumor formation rates and tumor growth were assessed by the number of mice forming tumors and three-dimension tumor sizes, respectively. There was no difference in tumor formation rates between fat-1 and wild type mice. TC-1 tumor sizes were plotted for 14 days in fat-1 and wild-type controls (Fig. 1). Tumor growth rates were consistently lower in fat-1 mice when compared to wild type mice at all time points. In fat-1 mice, tumor size at 14 days after injection was significantly smaller than in wild-type controls (Fig. 1). Although cell growth of TC-1 cells is dependent on HPV16 E6/E7 expression, E6 and E7 expression in TC-1 tumors was not downregulated in fat-1 mice (Fig. S1).

To further delineate mechanisms behind these differences in tumor growth in this model, particularly in terms of the possible role of host-derived cancer-associated stromal components including CAFs, we next examined whether omega-3 PUFAs modified angiogenesis in TC-1 tumor. We assessed semi-quantitatively tumor microvessel density in TC-1 tumors derived from fat-1 and wild type mice by counting the number of CD31-positive microvessels in immunohistochemical assay (Fig. 2A and 2B). CD31 immunostaining of TC-1 tumors derived from fat-1 and wild type mice (Fig. 2A) demonstrated hypovascularity of the fat-1-derived TC-1 tumors when compared with wild type-derived tumors. The number of CD31-positive microvessels per high-power field in fat-1 mice was significantly lower than that in wild type mice (Fig. 2B). These in vivo data indicated that TC-1 tumor growth and angiogenesis were at least suppressed in fat-1 mice when compared with wild type counterparts although it was difficult to accurately estimate TC-1 cell growth in fat-1 mice.

MMP-9 is downregulated in fat-1 mice-derived TC-1 tumors

To investigate potential differences in gene expression profiles of TC-1 tumors growing in the skin of fat-1 and wild type mice, TC-1 tumor tissues obtained from fat-1 and wild type mice were analyzed by cDNA microarray. Since omega-3 PUFAs are reported to influence cell proliferation and inflammation, Table 1 lists relative gene expression levels for representative genes associated with the tumor growth and inflammation (Table 1). With the exception of EGF, expression levels of almost all inflammatory cytokines/chemokines and growth factors in TC-1

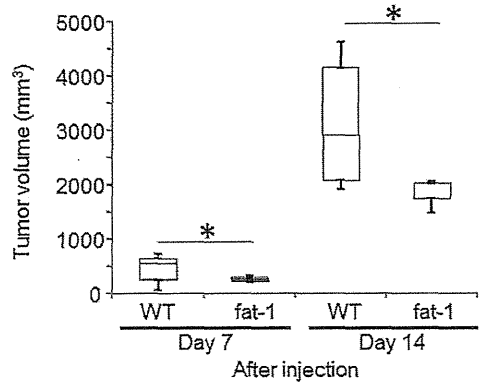

Figure 1. Tumor growth rates in fat-1 and wild type (WT) mice. 5×10^6 murine TC-1 cells suspended in 100 μl of DMEM were injected s.c. into each of 10 fat-1 and wild type mice. Tumor volume, based on caliper measurements, was calculated at 7 and 14 days after injection according to the following formula: (tumor volume) = 1/2×(the shortest diameter) ^{2}×(the largest diameter). Mean values with standard deviations are presented. Asterisks indicate those comparisons (fat-1 vs. wild type mice) with statistical significance ($p<0.05$).
doi:10.1371/journal.pone.0089605.g001

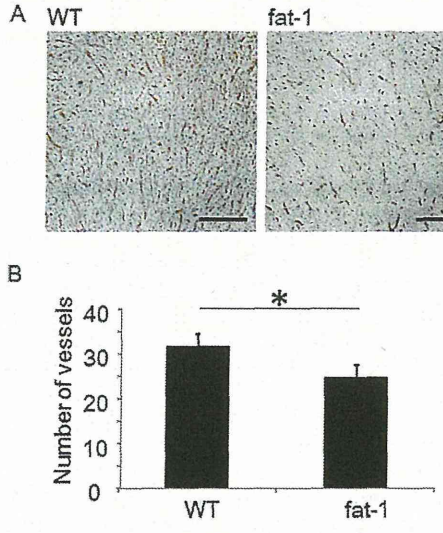

Figure 2. Omega-3 PUFAs suppress tumor vasculogenesis. CD31 immunostaining of the TC-1 tumor derived from wild type (WT) mice (A) and fat-1 (B). Bars indicate 200 μm. (C) Microvessel densities in TC-1 tumors are expressed as the representative number of labeled vessels in 4 fields (n = 5). Mean values with standard deviations are presented. Asterisks indicate those comparisons (fat-1 vs. wild type mice) with statistical significance ($p<0.05$).
doi:10.1371/journal.pone.0089605.g002

tumors from fat-1 mice were higher than those, in tumors from wild-type controls. This suggested that anti-inflammatory and anti-cell growth effects of omega-3 PUFAs are unlikely to be central to their anti-tumor activities, at least in this model. We next examined the expression of MMPs in these TC-1 tumors to further address stroma-related angiogenesis in the tumor micro-environments (Table 1). cDNA microarray demonstrated that the expression of MMP-2 and -9 were suppressed in fat-1 mice-derived TC-1 tumor while those of other MMPs were tended to be upregulated when compared to controls. To confirm these effects at the RNA level, RT-qPCR for MMP-9 was performed. MMP-9 RNA levels in fat-1 mice were approximately 60% lower than those in wild type controls (Fig. 3A). TC-1 tumor immunohisto-chemistry confirmed these results at the protein level. MMP-9 immunoreactivity in wild type mouse-derived TC-1 tumors was clearly stronger than fat-1 mouse-derived tumors (Fig. 3B). High power histochemical analysis of MMP-9 immnoreactivity in TC-1 cells (Fig. 3B, inserts) revealed negligible expression, while that of the stromal components including CAFs and endothelial cells was strongly positive only in the wild type-derived TC-1 tumors. These data indicated that the production of MMP-9 in CAFs and endothelial cells was clearly suppressed in fat-1 mice.

MMP-9 expression and gelatinase activity were suppressed in cultured primary fibroblasts derived from fat-1 mice

To mimic the cancer stromal microenvironment in vitro, we co-cultured fibroblasts isolated from fat-1 and wild type mice with TC-1 cells. We used lung tissues from fat-1 and wild type mice as the sources for fibroblasts, and differential adhesion methodology for their isolation. All fibroblasts were passaged 3–4 times prior to use in experiments. Baseline MMP-9 expression levels in primary fibroblasts from fat-1 mice were approximately 60% lower than those from wild type-derived fibroblasts (Fig. 4A). Culture

Table 1. Cytokine, growth factor, and MMP gene expression comparisons in TC-1 tumors from fat-1 vs wild type mice.

Genes	fat-1/WT ratio
EGF	**0.4**
CXCL-12	1.2
HGF	1.3
TGF-α	1.4
IL-6	2.0
IFN-γ	2.4
TNF-α	3.3
VEGF	3.7
IL-1β	12.0
MMP-9	**0.4**
MMP-2	**0.6**
MMP-7	1.9
MMP-1b	2.9
MMP-3	2.9
MMP-13	2.9
MMP-1a	3.6
MMP-16	4.1
MMP-10	11.6

doi:10.1371/journal.pone.0089605.t001

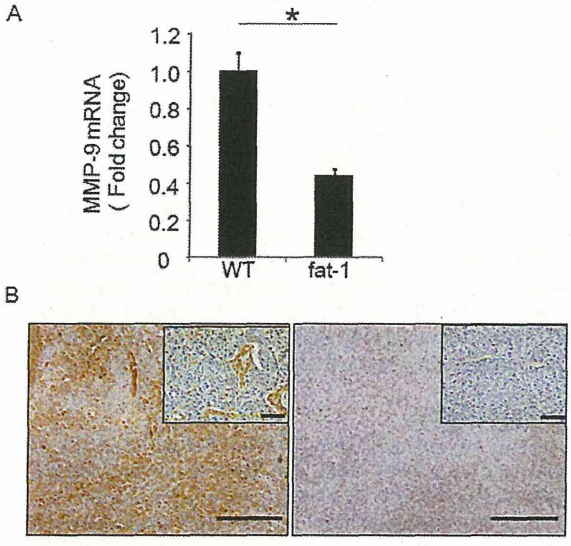

Figure 3. MMP-9 expression is downregulated in TC-1 tumors from fat-1 mice. Total RNA was extracted from TC-1 tumors, followed by reverse transcription. MMP-9 mRNA levels were measured by qRT-PCR. Expression levels of MMP-9 were normalized to β-actin as an internal standard (n = 4 in each group). Asterisks indicate those comparisons (fat-1 vs. wild type (WT) mice) with statistical significance ($p<0.05$). MMP-9 immunostaining of TC-1 tumors derived from wild type (WT) and fat-1 mice. Bars indicate 200 μm in low-power fields, 50 μm in high-power fields.
doi:10.1371/journal.pone.0089605.g003

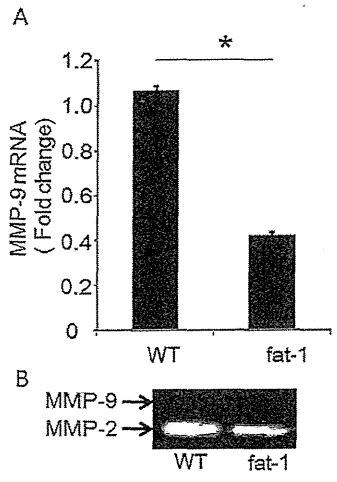

Figure 4. MMP-9 expression and enzymatic activity in primary-cultured fibroblasts. (A) Primary fibroblasts isolated from murine lungs were cultured. Total RNA from fibroblasts was reverse transcribed and MMP-9 mRNA levels were measured by qRT-PCR. Expression levels of MMP-9 were normalized to β-actin as an internal standard. Data are the representative of three independent experiments. The data were analyzed by using the Student's *t*-test. Asterisks indicate those comparisons (fat-1 vs. wild type (WT) mice) with statistical significance ($p<0.05$). (B) Gelatin zymography: Supernatant from primary fibroblast cultures were collected and separated by electrophoresis. Gelatinase activities were visualized by standard staining techniques.
doi:10.1371/journal.pone.0089605.g004

supernatants from each primary fibroblast subtype were collected and subjected to polyacrylamide gel electrophoresis to examine differences in MMP gelatinase activities (Fig. 4B). Using this method, MMP-2 was detected but MMP-9 was not in both fat-1 and wild type fibroblast

Next, these primary fibroblasts were co-cultured with TC-1 cells to examine fibroblasts activation upon in vitro exposure to cancer cells [11]. Fibroblasts and TC-1 cells were co-cultured for 24 hours and MMP-9 transcription was measured by RT-qPCR. Fibroblasts from fat-1 and from wild type mice increased demonstrated MMP-9 expression upon exposure to TC-1 cells (Fig. 5A). In fibroblasts derived from fat-1 mice, the extent of MMP-9 induction was lower than that in fibroblasts from wild type mice (Fig.5A). MMP-9 was not expressed in homotypic TC-1 cells, consistent with immunohistochemical data from our in vivo model. Furthermore, we confirmed that MMP-9 was not expressed in the TC-1 cells by using a transwell co-culture model (Fig. S2). Therefore, MMP-9 in the co-culture condition was derived not from TC-1 cells but from fibroblasts. MMP-2 gelatinase activity was detected in all cell culture conditions, including homotypic TC-1 cell cultures, and was not altered by co-culture conditions (Fig 5B, 5D). MMP-9 gelatinase activities were, however, detectable in fibroblast-TC-1 cell co-cultures, although MMP-9 gelatinase activity involving fat-1 fibroblasts was clearly suppressed when compared with wild type fibroblasts (Fig 5B, 5C), again supporting the concept that MMP-9 expression and gelatinase activity are suppressed by endogenous omega-3 PUFAs in CAFs derived from fat-1 mice.

Discussion

In this study, we examined the involvement of defined dietary factors (omega-3 and omega-6 PUFAs) in tumorigenesis using HPV-positive TC-1 cells and proposed a novel anti-tumor mechanism for omega-3 PUFAs that depends on the activities of CAFs. Omega-3 PUFAs have been shown to suppress cancer incidence and growth in various types of cancers [18,19,27]. Many studies have demonstrated that omega-3 PUFAs have these effects through anti-inflammatory responses directly and/or indirectly [25–27] as well as through inducing tumor cell apoptosis and/or suppressing tumor cell proliferation [18,19]. However, there have been few reports about the effects of omega-3 PUFAs on CAFs. CAFs have been implicated in facilitating the growth of several tumors by directly stimulating tumor cell proliferation and by enhancing angiogenesis [34,35]. Targeting genes and signaling pathways mediating interaction of CAFs and tumor-microenvironment are considered to be essential for development of new and effective cancer therapies [36,37]. In this study, using fat-1 mice and TC-1 tumor cells, we were able to clarify the effect of omega-3 PUFA-rich CAFs on tumorigenesis.

Many molecules, including growth factors, cytokines, and MMPs, play stimulatory and inhibitory roles in promoting angiogenesis [21]. We investigated gene expression of angiogenesis-related cytokines, growth factors and MMPs in the TC-1 tumors of fat-1 and wild type mice by cDNA microarray. The expression levels of almost all inflammatory cytokines/chemokines and growth factors in TC-1 tumors from fat-1 mice were higher than those in tumors from wild-type controls. In contrast, EGF and MMP-2 and -9 expression levels in fat-1 mice were lower than those in wild type mice. Since down-regulation of EGF in TC-1 tumors from fat-1 mice was predicted to promote TC-1 cell proliferation but tumor size in fat-1 mice was significantly smaller than in wild-type controls, we hypothesize that differences in MMP production between fat-1 and wild type mice may be responsible for the suppression of TC-1 tumor growth. Our in vitro data verified that MMP-9 derived from CAFs activated by TC-1 cell exposure was downregulated in the fat-1 mice. MMPs are reported to influence tumor progression by facilitating events pivotal for neovascularization and for the establishment of distant metastasis including proliferation, survival and migration of endothelial, tumor and stromal cells [8,9]. MMP inhibitors reduce angiogenesis, tumor number, and tumor growth, as does genetic ablation of MMP-9 [38]. In contrast to MMP-2, which is constitutively expressed, MMP-9 levels are usually low and enzyme expression is induced by cytokines that stimulate NF-κB [8,39]. Furthermore, elevated serum and tissue levels of MMP-9 are reported to be associated with cancer invasion and metastasis [40]. In breast cancer, MMP-9 activity has been localized around CAFs and CAFs co-cultured with cancer cells which secrete TGF-β, TNF-α, and other cytokines, increase production of MMP-9 [11], consistent with our in vitro data. In our data, suppression of MMP-9 would contribute to accompany hypo-angiogenesis in the tumor stromal component in fat-1 tumor.

Several transcription factors, including activator protein-1 (AP-1), Sp-1, and NF-κB, are reported to be involved in alterations in MMP-9 expression following exposure to various cytokines [41–43]. Conversely, several reports have demonstrated that omega-3 PUFAs have an inhibitory effect on the NF-κB pathway when activated by various stimuli [43–47]. Our own data suggest that activation of the NF-κB pathway upon co-culture with TC-1 cells may be suppressed by elevated level of omega-3 PUFAs in fibroblast obtained from fat-1 mice.

In our experiments, we consistently used primary fibroblasts that had been passaged 3-4 times only. Nevertheless, lipid mediator analysis of the fibroblasts revealed that those derived from fat-1 mice produced larger amounts of omega-3 PUFAs including EPA-derived metabolites when compared with those

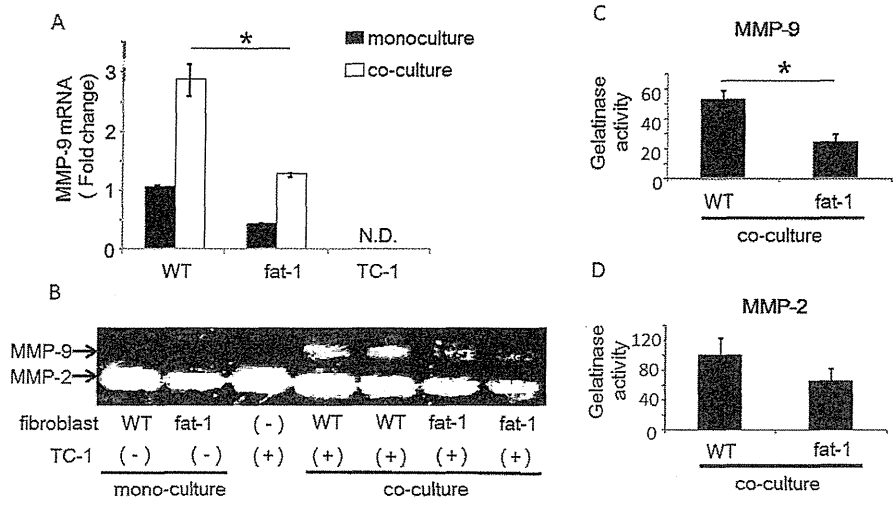

Figure 5. The increased MMP-9 expression and activity in TC-1/fibroblast co-cultures is inhibited in fat-1 mice. (A) Isolated fibroblasts were co-cultured with TC-1 cells for 24 hours and expression levels of MMP-9 in the fibroblasts were measured by RT-qPCR. Expression levels of MMP-9 were normalized to β-actin as an internal standard. The data are representative of three independent experiments. The data were analyzed using the Student's *t*-test. Asterisks indicate those comparisons (fat-1 vs. wild type (WT) mice) with statistical significance ($p<0.05$). "N.D." indicates 'not detected'. (B) Gelatin zymography: Supernatants from fibroblast homotypic cultures and fibroblast/TC-1 co-cultures were collected and separated by electrophoresis. Gelatinase activities were visualized by standard staining techniques. (C, D) For semi-quantitative analyses, gelatin zymography bands were analyzed using image analysis software. Results are represented as mean ±SEM of three independent experiments. The data were analyzed using the Student's *t*-test. Asterisks indicate those comparisons (fat-1 vs. wild type (WT) mice) with statistical significance ($p<0.05$).
doi:10.1371/journal.pone.0089605.g005

derived from wild type controls (Fig.S3), confirming that the cultured fibroblasts retained the characteristic to make omega-3 PUFA rich environment.

TC-1 tumor microarray data showed that several inflammatory cytokines/chemokines and growth factors were upregulated in fat-1 mice. However, the data indicated gene expression levels in both TC-1 cells and stromal components, including fibroblasts, endothelial and immune cells. Therefore, expression levels of each cytokine/chemokine were dependent on their primary sources of production. MMP-9 was produced by the fibroblasts derived from fat-1 mice but not by TC-1 cells. Therefore, suppression of the NF-κB pathway by elevated levels of omega-3 PUFAs in fat-1-derived stromal components may have a specific and potent effect on MMP-9 expression levels when compared with the other inflammatory cytokines/chemokines. On the other hand, a previous study demonstrates that omega-3 PUFAs activate NK cells and increase proportions of activated CD8+ cells; this is followed by enhanced anti-tumor effects [48]. Therefore, omega-3 PUFAs may exert both anti-inflammatory and pro-inflammatory effects on immune cells.

In this study, we have demonstrated that an omega-3 PUFAs-rich microenvironment can suppress MMP-9 secretion from CAFs and that this is associated with subsequent tumor hypo-angiogenesis. This study proposes a novel anti-tumor effect of omega-3 PUFAs by modulating tumor microenvironment especially on CAFs.

Supporting Information

Figure S1 Expression levels of E6 and E7 mRNA in TC-1 tumor. Total RNA was extracted from TC-1 tumors, followed by reverse transcription. E6 and E7 mRNA levels were measured by qRT-PCR. Expression levels of E6 and E7 mRNA were normalized to β-actin as an internal standard. The E6 primers were forward, 5'- TGCACAGAGCTGCAAACAAC -3', and reverse, 5'- AGCATATGGATTCCCATCTC -3'. The E7 primers were forward, 5'- TTTGCAACCAGAGACAACTGA -3', and reverse, 5'- GCCCATTAACAGGTCTTCCA -3'.
(TIF)

Figure S2 MMP-9 mRNA was not induced from TC-1 cells by co-culture with fibroblasts. 150 μL of suspensions (2×10^6/mL) of TC-1 cells or fibroblasts were added to the upper chamber, 500 μL of suspensions (1×10^5/mL) of TC-1 cells or fibroblasts were added to the lower chamber of the 24 well Transwell plates (1 μm pore) and placed in an incubator with 5% CO_2 at 37°C for 24 h and expression levels of MMP-9 in the TC-1 or fibroblasts in the lower chamber were measured by RT-qPCR. N.D. indicates 'not detected'.
(TIF)

Figure S3 Lipid mediator analysis of fibroblast/TC-1 co-cultured medium. Supernatants from fibroblast/TC-1 co-cultures were collected and LC-MS/MS-based mediator lipidomics was performed on Acquity UPLC BEH C_{18} column (1.0 mm×150 mm×1.7 μm) using Acquity UltraPerformance LC system (Waters Co.) coupled to an electrospray (ESI) triple quadrupole mass spectrometer (QTRAP5500; AB SCIEX). The MS/MS analyses were performed in negative ion mode, and the eicosanoids and docosanoids were identified and quantified by multiple reaction monitoring. Calibration curves between 1 and 1000 pg and the LC retention times for each compounds were constructed with synthetic standards.
(TIF)

Acknowledgments

We gratefully thank Dr. Danny J. Schust for careful editing of the manuscript and Dr. Terufumi Yokoyama for excellent comments and advice on experiments using murine models.

Author Contributions

Conceived and designed the experiments: AT K. Kawana KT AY MA K. Koga. Performed the experiments: AT K. Kawana KT AY YI KN TI HN SK YM. Analyzed the data: AT K. Kawana KT AY K. Koga TA KA OW KO HA MA JK TF YO. Contributed reagents/materials/analysis tools: AT KT AY. Wrote the paper: AT K. Kawana MA.

References

1. Lorusso G, Ruegg C (2008) The tumor microenvironment and its contribution to tumor evolution toward metastasis, Histochem Cell Biol, 130:1091–1103
2. Joyce JA, Pollard JW (2009) Microenvironmental regulation of metastasis, Nat Rev Cancer, 9:239–252
3. Franco OE, Shaw AK, Strand DW, Hayward SW (2010) Cancer associated fibroblasts in cancer pathogenesis, Semin Cell Dev Biol, 21:33–39
4. Kalluri R, Zeisberg M (2006) Fibroblasts in cancer, Nat Rev Cancer, 6:392–401
5. Schauer IG, Zhang J, Xing Z, Guo X, Mercado-Uribe I, et al (2013) Interleukin-1beta promotes ovarian tumorigenesis through a p53/NF-kappaB-mediated inflammatory response in stromal fibroblasts, Neoplasia, 15:409–420
6. Zhu Y, Zhu M, Lance P (2012) IL1beta-mediated Stromal COX-2 signaling mediates proliferation and invasiveness of colonic epithelial cancer cells, Exp Cell Res, 318:2520–2530
7. Jones CB, Sane DC, Herrington DM (2003) Matrix metalloproteinases, Cardiovas Res, 59:812–823
8. Lynch CC, Matrisian LM (2002) Matrix metalloproteinases in tumor-host cell communication, Differentiation, 70:561–573
9. Chantrain CF, Shimada H, Jodele S, Groshen S, Ye W, et al (2004) Stromal Matrix Metalloproteinase-9 Regulates the Vascular Architecture in Neuroblastoma by Promoting Pericyte Recruitment, Cancer Res, 64:1675–1686
10. Roomi MW, Monterrey JC, Kalinovsky T, Niedzwiecki A, Rath M (2009) Modulation of MMP-2 and MMP-9 by cytokines, mitogens and inhibitors in lung cancer and malignant mesothelioma cell lines, Oncol Rep, 22:1283–1291
11. Stuelten CH, Byfield SD, Arany PR, Karpova TS, Stetler-Stevenson WG, et al (2005) Breast cancer cells induce stromal fibroblasts to express MMP-9 via secretion of TNF-α and TGF-β, Journal of Cell Sci, 118:2143–2153
12. Generscb E, Hayess K, Neuenfeld Y, Haller H (2000) Sustained ERK phosphorylation is necessary but not sufficient for MMP-9 regulation in endothelial cells: involvement of Ras-dependent and -independent pathways, J Cell Sci, 113 Pt 23:4319–4330
13. Heissig B, Hattori K, Friedrich M, Rafii S, Werb Z (2003) Angiogenesis: vascular remodeling of the extracellular matrix involves metalloproteinases, Current Opinion in Hematol, 10:136–141
14. Serhan CN, Savill J (2005) Resolution of inflammation: the beginning programs the end, Nat Immunol, 6:1191–1197
15. Hardman WE (2002) Omega-3 fatty acids to augment cancer therapy, J Nutr, 132:3508S–3512S
16. Lee CY, Sit WH, Fan ST, Man K, Jor IW, et al (2010) The cell cycle effects of docosahexaenoic acid on human metastatic hepatocellular carcinoma proliferation, Int J Oncol, 36:991–998
17. Habermann N, Schon A, Lund EK, Glei M (2010) Fish fatty acids alter markers of apoptosis in colorectal adenoma and adenocarcinoma cell lines but fish consumption has no impact on apoptosis-induction ex vivo, Apoptosis, 15:621–630
18. Serini S, Piccioni E, Merendino N, Calviello G (2009) Dietary polyunsaturated fatty acids as inducers of apoptosis: implications for cancer, Apoptosis, 14:135–152
19. Field CJ, Schley PD (2004) Evidence for potential mechanisms for the effect of conjugated linoleic acid on tumor metabolism and immune function: lessons from n-3 fatty acids, Am J Clin Nutr, 79:1190S–1198S
20. Calviello G, Di Nicuolo F, Gragnoli S, Piccioni E, Serini S, et al (2004) n-3 PUFAs reduce VEGF expression in human colon cancer cells modulating the COX-2/PGE2 induced ERK-1 and -2 and HIF-1α induction pathway, Carcinogenesis, 25:2303–2310
21. Spencer L, Mann C, Metcalfe M, Webb MB, Pollard C, et al (2009) The effect of omega-3 FAs on tumour angiogenesis and their therapeutic potential, Eur j cancer, 45:2077–2086
22. Rose DP, Connolly JM (1999) Antiangiogenicity of docosahexaenoic acid and its role in the suppression of breast cancer cell growth in nude mice, Int J Oncol, 15:1011–1015
23. Mukutmoni-Norris M, Hubbard NE, Erickson KL (2000) Modulation of murine mammary tumor vasculature by dietary n-3 fatty acids in fish oil, Cancer Lett, 150:101–109
24. Tevar R, Jho DH, Babcock T, Helton WS, Espat NJ (2002) Omega-3 fatty acid supplementation reduces tumor growth and vascular endothelial growth factor expression in a model of progressive non-metastasizing malignancy, JPEN J Parenter Enteral Nutr, 26:285–289
25. Kang JX (2007) Fat-1 transgenic mice: a new model for omega-3 research, Prostaglandins Leukot Essent Fatty Acids, 77:263–267
26. Kang JX, Wang J, Wu L, Kang ZB (2004) Transgenic mice: fat-1 mice convert n-6 to n-3 fatty acids, Nature, 427:504
27. Xia S, Lu Y, Wang J, He C, Hong S, et al (2006) Melanoma growth is reduced in fat-1 transgenic mice: Impact of omega-6/omega-3 essential fatty acids, PNAS, 103:12499–12504
28. Nowak J, Weylandt KH, Habbel P, Wang J, Dignass A, et al (2007) Colitis-associated colon tumorigenesis is suppressed in transgenic mice rich in endogenous n-3 fatty acids, Carcinogenesis, 28:1991–1995
29. Jia Q, Lupton JR, Smith R, Weeks BR, Callaway E, et al (2008) Reduced Colitis-Associated Colon Cancer in Fat-1 (n-3 Fatty Acid Desaturase) Transgenic Mice, Cancer Res, 68:3985–3991
30. Weylandt KH, Krause LF, Gomolka B, Chiu C-Y, Bilal S, et al (2011) Suppressed liver tumorigenesis in fat-1 mice with elevated omega-3 fatty acids is associated with increased omega-3 derived lipid mediators and reduced TNF-α, Carcinogenesis, 32:897–903
31. zur Hausen H (2009) Papillomaviruses in the causation of human cancers — a brief historical account, Virology, 384:260–265
32. Lin KY, Guarnieri FG, Staveley-O'Carroll KF, Levitsky HI, August JT, et al (1996) Treatment of established tumors with a novel vaccine that enhances major histocompatibility class II presentation of tumor antigen, Cancer Res, 56:21–26
33. Rowe RG, Keena D, Sabeh F, Willis AL, Weiss SJ (2011) Pulmonary fibroblasts mobilize the membrane-tethered matrix metalloprotease, MT1-MMP, to destructively remodel and invade interstitial type I collagen barriers, Am J Physiol Lung Cell Mol Physiol, 301:L683–692
34. Erez N, Truitt M, Olson P, Arron ST, Hanahan D (2010) Cancer-Associated Fibroblasts Are Activated in Incipient Neoplasia to Orchestrate Tumor-Promoting Inflammation in an NF-kappaB-Dependent Manner, Cancer Cell, 17:135–147
35. Bhowmick NA, Neilson EG, Moses HL (2004) Stromal fibroblasts in cancer initiation and progression, Nature, 432:332–337
36. Hanahan D, Coussens LM (2012) Accessories to the crime: functions of cells recruited to the tumor microenvironment, Cancer Cell, 21:309–322
37. Valastyan S, Weinberg RA (2011) Tumor metastasis: molecular insights and evolving paradigms, Cell, 147:275-292
38. Bergers G, Brekken R, McMahon G, Vu TH, Itoh T, et al (2000) Matrix metalloproteinase-9 triggers the angiogenic switch during carcinogenesis, Nat Cell Biol, 2:737–744
39. Sternlicht MD, Werb Z (2001) How matrix metalloproteinases regulate cell behavior, Annu Rev Cell Dev Biol, 17:463–516
40. Nabeshima K, Inoue T, Shimao Y, Sameshima T (2002) Matrix metalloproteinases in tumor invasion: role for cell migration, Pathol Int, 52:255–264
41. Kupferman ME, Fini ME, Muller WJ, Weber R, Cheng Y, et al (2000) Matrix metalloproteinase 9 promoter activity is induced coincident with invasion during tumor progression, Am J Pathol, 157:1777–1783
42. Simon C, Simon M, Vucelic G, Hicks MJ, Plinkert PK, et al (2001) The p38 SAPK pathway regulates the expression of the MMP-9 collagenase via AP-1-dependent promoter activation, Exp Cell Res, 271:344–355
43. Kim HH, Lee Y, Eun HC, Chung JH (2008) Eicosapentaenoic acid inhibits TNF-alpha-induced matrix metalloproteinase-9 expression in human keratinocytes, HaCaT cells, Biochem Biophys Res Commun, 368:343–349
44. Mishra A, Chaudhary A, Sethi S (2004) Oxidized omega-3 fatty acids inhibit NF-kappaB activation via a PPARalpha-dependent pathway, Arterioscler Thromb Vasc Biol, 24:1621–1627
45. Dichtl W, Ares MP, Jonson AN, Jovinge S, Pachinger O, et al (2002) Linoleic acid-stimulated vascular adhesion molecule-1 expression in endothelial cells depends on nuclear factor-kappaB activation, Metabolism, 51:327–333
46. Zhao Y, Joshi-Barve S, Barve S, Chen LH (2004) Eicosapentaenoic acid prevents LPS-induced TNF-alpha expression by preventing NF-kappaB activation, J Am Coll Nutr, 23:71–78
47. Ross JA, Maingay JP, Fearon KC, Sangster K, Powell JJ (2003) Eicosapentaenoic acid perturbs signalling via the NFkappaB transcriptional pathway in pancreatic tumour cells, Int J Oncol, 23:1733–1738
48. Robinson LE, Clandinin MT, Field CJ (2002) The role of dietary long-chain n-3 fatty acids in anti-cancer immune defense and R3230AC mammary tumor growth in rats: influence of diet fat composition, Breast Cancer Res Treat, 73:145–160

THE JOURNAL OF
Obstetrics and Gynaecology Research

doi:10.1111/jog.12235 J. Obstet. Gynaecol. Res. Vol. 40, No. 3: 869–872, March 2014

Poor prognosis of ovarian cancer with large cell neuroendocrine carcinoma: Case report and review of published works

Kayo Asada[1,2], Kei Kawana[1], Shinichi Teshima[3], Ako Saito[2], Masakiyo Kawabata[2] and Tomoyuki Fujii[1]

[1]*Department of Obstetrics and Gynecology, Faculty of Medicine, The University of Tokyo,* [2]*Department of Obstetrics and Gynecology, The Fraternity Memorial Hospital, Tokyo, and* [3]*Department of Pathology, The Fraternity Memorial Hospital, Sumida-ku, Japan*

Abstract

Large cell neuroendocrine carcinoma (LCNEC) is well-reported to result in unfavorable prognoses in many organ cancers while being rarely reported in gynecologic cancer, especially ovarian and endometrial cancers. Here we report a case of ovarian cancer with LCNEC which spread to distant organs within 1 year of primary surgery despite the fact that the post-surgical stage was Ia. The case received platinum-based chemotherapy as an adjuvant therapy after her curative surgery. However, LCNEC in the case was resistant to the chemotherapy. In our review of published works, ovarian cancer cases with LCNEC show poor prognoses regardless of adjuvant chemotherapy following complete resection. Median overall survival was 10 months in stage I cases. Development of chemotherapy sensitive for LCNEC is needed.

Key words: chromogranin A, gynecologic cancer, large cell neuroendocrine carcinoma, ovarian cancer, platinum-based chemotherapy.

Introduction

Large cell neuroendocrine carcinoma (LCNEC) is synonymous with 'undifferentiated carcinoma of non-small cell neuroendocrine type' and defined as 'a malignant tumor composed of large cells that show neuroendocrine differentiation'.[1] However, there exist no generally accepted criteria for neuroendocrine tumor differentiation, which usually depends on a combination of typical structural, immunohistochemical and ultrastructural findings. World Health Organization (WHO) criteria describe that LCNEC of the lung is characterized by positive immunostaining for chromogranin A, synaptophysin or CD56 (N-CAM) and at least one of them is enough if the staining is clear cut.[2] LCNEC of the ovary is very rare and only 35 cases have been reported previously worldwide.[2–17] Its prognosis is generally very poor, even when the diagnosis is made at an early stage. We experienced a case of LCNEC of the ovary who died of disseminated disease within 7 months after the primary surgery despite extensive surgery and adjuvant chemotherapy.

Case Report

A 50-year-old woman, gravida 3 para 2, presented with abdominal distension for 1 month. Physical

Received: April 2 2013.
Accepted: July 8 2013.
Reprint request to: Professor Kei Kawana, Department of Obstetrics and Gynecology, Graduate School of Medicine, The University of Tokyo, 7-3-1 Hongo, Bunkyo-ku, Tokyo 113-8655, Japan. Email: kkawana-tky@umin.org
Conflict of interest: We have no relationships with companies that may have a financial interest in the information contained in the manuscript.

examination revealed a firm mass in the lower abdomen that was equivalent to the head of a newborn infant. Ultrasonographic tomography, magnetic resonance imaging and computed tomography (CT) demonstrated a monolocular cyst measuring 15 cm × 12 cm × 10 cm in diameter in the abdominal cavity. Abdominal organs were otherwise normal and the lungs were normal. Preoperative serum level of carbohydrate antigen (CA)125, CA19-9, carcinoembryonic antigen, α-fetoprotein and lactate dehydrogenase were within normal ranges. A smooth-surfaced right ovarian tumor was found at laparotomy. The uterus, tubes, left ovary and omentum were normal and no other tumor was evident in the abdominal cavity. Total abdominal hysterectomy, bilateral salpingo-oophorectomy, omentectomy and pelvic lymphadenectomy were performed. A smooth round tumor 15 cm in diameter was resected without rupture. In the tumor wall, several thickened lesions were seen (Fig. 1a, arrowhead). Hematoxylin–eosin staining of the tumor revealed microscopically mucinous epithelium lining the inside of the tumor wall and several parts relevant to the thickened lesions were composed of poorly differentiated large cells forming a front of the normal mucinous epithelium (Fig. 1b,c). To assess features of the large cells, immunohistochemistry was performed. Positivity for CD56, chromogranin A, synaptophysin and neuron-specific enolase (NSE) demonstrated the large cells were neuroendocrine components (Fig. 1d–g). Taken together, the ovarian tumor was classified as LCNEC associated with mucinous adenoma. Remarkable vascular invasion was observed in the tumor wall, especially around the thickened lesions.

She was diagnosed as having ovarian cancer of stage Ia (pT1aN0M0) of LCNEC associated with mucinous adenoma and received EP (cisplatin 75 mg/m^2 and etoposide 100 mg/m^2 once a day for 5 days) as an adjuvant chemotherapy. However, multiple liver metastases were detected by CT at 4 months after her primary operation when she received three rounds of EP. Then, her chemotherapy regimen was changed to TC (paclitaxel 175 mg/m^2 and carboplatin AUC 6) or CPT-11 (90 mg/m^2) alone as second- or third-line chemotherapy, respectively. Clinical responses to any regimen were not observed in this case. Her cancer was thought to be refractory for any regimen and progressed rapidly. Unfortunately, she died of progressive disease only 7 months after her primary operation.

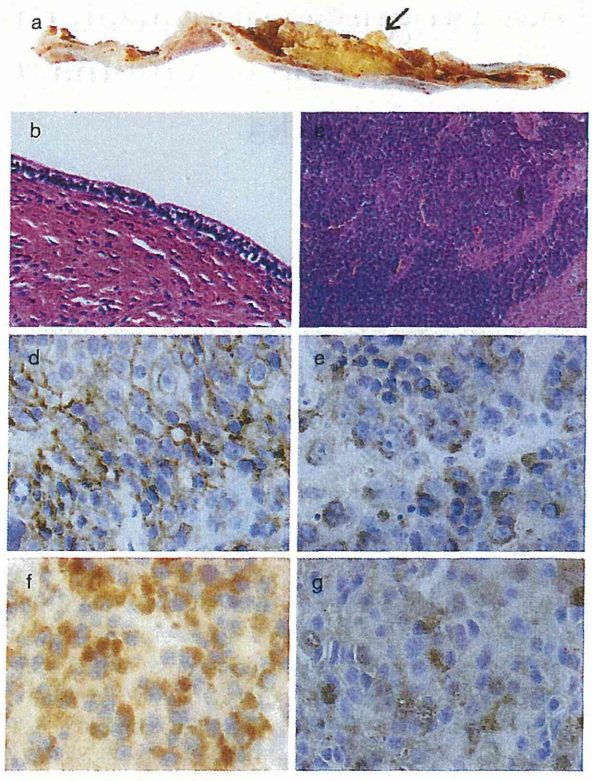

Figure 1 Pathological and immunohistochemical findings of this case. (a) Macroscopic finding: the cut surface of the right ovary was smooth. Several thickened lesions were seen in the tumor wall (arrow). (b) Microscopic finding (hematoxylin–eosin [HE] staining): mucinous epithelium lined inside of the tumor wall (original magnification, ×100). (c) Microscopic finding (HE staining): poorly-differentiated large cells in several parts relevant to the thickened lesions (×40). (d–g) Immunohistochemical studies of this case for representative neuroendocrine markers: CD56 (d: ×400), chromogranin A (e: ×400), synaptophysin (f: ×400) and neuron-specific enolase (g: ×400).

Discussion

Large cell neuroendocrine carcinoma of the ovary is included in the WHO tumor classification. To date, 35 cases of ovarian LCNEC have been reported in the published work. Thirty-three cases received an operation and been diagnosed postoperatively as ovarian LCNEC. These included 16 cases of stage I, three cases of stage II, eight cases of stage III and six cases of stage IV. Most of these cases seem to be associated with benign ovarian epithelial neoplasms. Of 33 cases, pure neuroendocrine carcinoma accounted for only four

cases while the remaining neuroendocrine carcinomas coexisted with ovarian epithelial tumors or germ cell tumors.

The tumor in our case was lined with benign epithelium mucinous adenoma. On the other hand, most of the tumor consisted of a poorly differentiated component of large tumor cells exhibiting proliferation in the thickened wall. Nuclei were large and had prominent nucleoli. Vascular invasion was prominent. Immunohistochemistry revealed that the cells of the poorly differentiated component were diffusely positive for CD56, chromogranin A, synaptophysin and NSE. Taken together, the tumor fulfilled the histopathological criteria for a neuroendocrine carcinoma.[2]

A high frequency of vascular invasion has been reported in neuroendocrine carcinomas of the lung and other sites.[18] In terms of gynecologic cancer, vascular invasion in LCNEC of the cervix has been reported to be much more common than in other types of cervical carcinomas.[19] Our case showed a definite vascular invasion at the lesions of LCNEC, which might have resulted in the distant metastasis in spite of the early stage.

Large cell neuroendocrine carcinoma in any organs is thought to be an aggressive tumor with high mortality despite extensive surgery and adjuvant chemotherapy. In our case, LCNEC spread to distant organs within 1 year after primary surgery despite the fact that the post-surgical stage was Ia and adjuvant chemotherapy was performed. However, one report mentions that cases of ovarian LCNEC, particularly those of stage I and/or those who have received platinum-based therapy, may have a favorable prognosis.[13] Then, we addressed the overall survival rate with ovarian LCNEC of stage I by Kaplan–Meier curve based on the published works (Fig. 2). Overall survival was available in 15 previously reported cases, with a median follow-up period of 9 months (including our study). Among these 16 cases, nine died of the disease within 3–19 months after primary operation and the remaining seven patients were alive at follow-up periods ranging 6–120 months. The median overall survival was 10 months and 1-year overall survival rate was 47.1% on the Kaplan–Meier curve. This suggests that the LCNEC of the ovary has a very poor prognosis even at stage I.

Veronesi *et al.* reported a series of 144 cases of lung LCNEC who received debulking surgery. Of them, 21 and 24 cases received neoadjuvant or postoperative adjuvant chemotherapy, respectively, and response rate of the chemotherapy was 80% in 15 cases with data

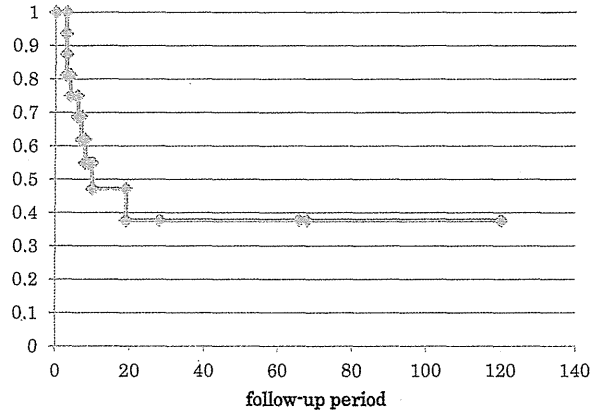

Figure 2 Kaplan–Meier curve of overall survival for ovarian large cell neuroendocrine carcinoma stage I. This case and 15 cases reported as stage I in the published work are summarized. One-year overall survival of these cases was 47.1% by Kaplan–Meier method. ⟷, survival rate.

available. They demonstrated that combination of chemotherapy and surgery improved overall survival of the lung LCNEC stage I with marginal significance when compared with surgery alone.[20] Another group also reported that two cases of lung stage I LCNEC who received cisplatin and etoposide combination chemotherapy survived for 2 and 5 years after complete pulmonary resection, respectively.[21] These data allowed for a possibility that platinum-based adjuvant chemotherapy after curative surgery may result in relatively long survival of the lung LCNEC cases of early stage. These rationales encouraged us to add combination adjuvant chemotherapy of cisplatin and etoposide to our case. However, our case died of disseminated disease within 7 months of the primary surgery. Chemosensitivity of the ovarian LCNEC to platinum-based chemotherapy may be lower than that of the lung LCNEC. Additional cases of this carcinoma will have to be collected to establish optimal adjuvant chemotherapy.

Acknowledgment

We are grateful to Dr Daichi Maeda for his pathological review and excellent comments and to Dr Minagawa for immunohistochemical techniques.

References

1. Roth LM, Tsubara A, Dietel M, Senzaki H. Miscellaneous tumors and tumor-like conditions of the ovary. In: Tavassoli

FA, Devilee P (eds). *Pathology and Genetics of Tumours of the Breast and Female Genital Organs. World Health Organization Classification of Tumors*. Lyon: IARC Press, 2003; 182–190.
2. Tsuji T, Togami S, Shintomo N, Fukamachi N, Douchi T, Taguchi S. Ovarian large cell neuroendocrine carcinoma. *J Obstet Gynaecol Res* 2008; **34** (4 Pt 2): 726–730.
3. Collins RJ, Cheung A, Ngan HY, Wong LC, Chan SY, Ma HK. Primary mixed neuroendocrine and mucinous carcinoma of the ovary. *Arch Gynecol Obstet* 1991; **248**: 139–143.
4. Khurana KK, Tornos C, Silva EG. Ovarian neuroendocrine carcinoma associated with a mucinous neoplasm. *Arch Pathol Lab Med* 1994; **118**: 1032–1034.
5. Eichhorn JH, Lawrence WD, Young RH, Scully RE. Ovarian neuroendocrine carcinomas of non-small-cell type associated with surface epithelial adenocarcinomas. A study of five cases and review of the literature. *Int J Gynecol Pathol* 1996; **15**: 303–314.
6. Jones K, Diaz JA, Donner LR. Neuroendocrine carcinoma arising in an ovarian mucinous cystadenoma. *Int J Gynecol Pathol* 1996; **15**: 167–170.
7. Chen KT. Composite large-cell neuroendocrine carcinoma and surface epithelial-stromal neoplasm of the ovary. *Int J Surg Pathol* 2000; **8**: 169–174.
8. Behnam K, Kabus D, Behnam M. Primary ovarian undifferentiated non-small cell carcinoma, neuroendocrine type. *Gynecol Oncol* 2004; **92**: 372–375.
9. Ohira S, Itoh K, Shiozawa T *et al.* Ovarian NSCNEC with paraneoplastic parathyroid hormone-related hypercalcemia. *Int J Gynecol Pathol* 2004; **23**: 393–397.
10. Ahmed Z, Aftab K, Kayani N. Ovarian primary neuroendocrine carcinoma of non-small cell type: Report of an extremely rare neoplasm. *J Pak Med Assoc* 2005; **55**: 82–84.
11. Choi YD, Lee JS, Choi C, Park CS, Nam JH. Ovarian neuroendocrine carcinoma, non-small cell type, associated with serous carcinoma. *Gynecol Oncol* 2007; **104**: 747–752.
12. Lindboe CF. Large cell neuroendocrine carcinoma of the ovary. *APMIS* 2007; **115**: 169–176.
13. Veras E, Deavers MT, Silva EG, Malpica A. Ovarian nonsmall cell neuroendocrine carcinoma: A clinicopathologic and immunohistochemical study of 11 cases. *Am J Surg Pathol* 2007; **31**: 774–782.
14. Dundr P, Fischerova D, Povysil C, Cibula D. Primary pure large-cell neuroendocrine carcinoma of the ovary. *Pathol Res Pract* 2008; **204**: 133–137.
15. Chenevert J, Bessette P, Plante M, Tetu B, Dube V. Mixed ovarian large cell neuroendocrine carcinoma, mucinous adenocarcinoma, and teratoma: A report of two cases and review of the literature. *Pathol Res Pract* 2009; **205**: 657–661.
16. Yasuoka H, Tsujimoto M, Fujita S *et al.* Monoclonality of composite large cell neuroendocrine carcinoma and mucinous epithelial tumor of the ovary: A case study. *Int J Gynecol Pathol* 2009; **28**: 55–58.
17. Hirasawa T. Ovarian neuroendocrine carcinoma associated with mucinous carcinoma and teratoma. *Nippon Rinsho*. 2004; **62**: 973–978.
18. Tsuchiya T, Akamine S, Muraoka M *et al.* Stage IA non-small cell lung cancer: Vessel invasion is a poor prognostic factor and a new target of adjuvant chemotherapy. *Lung Cancer*. 2007; **56**: 341–348.
19. Sato Y, Shimamoto T, Amada S, Asada Y, Hayashi T. Large cell neuroendocrine carcinoma of the uterine cervix: A clinicopathological study of six cases. *Int J Gynecol Pathol* 2003; **22**: 226–230.
20. Veronesi G, Morandi U, Alloisio M *et al.* Large cell neuroendocrine carcinoma of the lung: A retrospective analysis of 144 surgical cases. *Lung Cancer*. 2006; **53**: 111–115.
21. Iyoda A, Hiroshima K, Moriya Y *et al.* Prospective study of adjuvant chemotherapy for pulmonary large cell neuroendocrine carcinoma. *Ann Thorac Surg* 2006; **82**: 1802–1807.

THE JOURNAL OF
Obstetrics and Gynaecology Research

doi:10.1111/jog.12196 J. Obstet. Gynaecol. Res. Vol. 40, No. 2: 554–560, February 2014

High-risk human papillomavirus correlates with recurrence after laser ablation for treatment of patients with cervical intraepithelial neoplasia 3: A long-term follow-up retrospective study

Kanako Inaba, Kazunori Nagasaka, Kei Kawana, Takahide Arimoto, Yoko Matsumoto, Tetsushi Tsuruga, Mayuyo Mori-Uchino, Shiho Miura, Kenbun Sone, Katsutoshi Oda, Shunsuke Nakagawa, Tetsu Yano, Shiro Kozuma and Tomoyuki Fujii

Department of Obstetrics and Gynecology, Faculty of Medicine, The University of Tokyo, Tokyo, Japan

Abstract

Aim: The purpose of our study was to evaluate the efficacy of laser ablation as a conservative treatment for cervical intraepithelial neoplasia 3 (CIN3) and assess whether the human papillomavirus (HPV) test is useful to predict recurrence after treatment.

Materials and Methods: A total of 134 patients who received laser ablation for treatment of CIN3 were enrolled in this study. During the follow-up period, patients were followed with cytological and colposcopic evaluations. Recurrence of CIN3 was regarded as the primary end-point. HPV genotype was tested before and after treatment. Post-treatment cumulative recurrence rates were estimated and comparisons by both patient age and HPV genotype were performed.

Results: Overall cumulative recurrence rate of CIN3 in the first year after treatment was 22.6% for all patients. No significant correlation was shown between patient age and recurrence. Patients infected by specific genotypes (16, 18, 31, 33, 52, and 58) frequently failed to clear the infection after treatment. The 1-year recurrence-free survival in those positive after treatment for eight high-risk genotypes (16, 18, 31, 33, 35, 45, 52, and 58) was significantly lower (66.7%), compared to that in those positive for other high-risk types (78.6%). The recurrence-free survival of those who remained HPV-positive after treatment was significantly lower than those who turned negative.

Conclusion: Laser ablation should be performed prudently with appropriate patient counseling about recurrence rate. Considering its minimal invasiveness, laser ablation is effective, especially for young patients who are negative for eight high-risk genotypes. With regard to HPV testing, although genotyping has significant value for predicting recurrence, screening for all genotypes warrants further evaluation.

Key words: cervical intraepithelial neoplasia 3, human papillomavirus testing, laser ablation, recurrence, treatment efficacy.

Introduction

The spread of systematic screening programs has detected more cervical intraepithelial neoplasia (CIN) and has succeeded in producing marked declines in cervical carcinoma incidence and mortality in the developed countries where screening programs and treatment for pre-invasive lesions are

Received: January 9 2013.
Accepted: May 27 2013.
Reprint request to: Dr Kazunori Nagasaka, Department of Obstetrics and Gynecology, Faculty of Medicine, The University of Tokyo, 7-3-1 Hongo, Bunkyo-ku, Tokyo 113-8655, Japan. Email: nagasakak-tky@umin.ac.jp

widespread. Many women who receive treatment for high-grade CIN are of reproductive age with a mean age of approximately 30 years old.[1] Therefore, the treatment should not only be effective but also have minimum adverse effects on future fertility and obstetrical outcomes. Cold-knife conization, laser conization, loop electrosurgical excisional procedure (LEEP), cryotherapy, and laser ablation are all conservative methods used to treat high-grade CIN by removing or destroying the transformation zone containing abnormal epithelial cells and thereby preserving cervical function. According to data from the Japan Society of Obstetrics and Gynecology (JSOG), conservative conization methods were chosen for only 33% of women with carcinoma *in situ* (CIS) in 1990, for which hysterectomy had been the treatment standard, rising as high as 79.3% in 2009. These data robustly represent the increasing demand for conservative CIN treatments at the present time.

Many studies have demonstrated that these methods show similarly low morbidity and are equally successful at preventing invasive cervical cancer.[2–5] Of these conservative methods, characteristics of laser ablation have been well reported due to its fertility-sparing advantage. Laser ablation is usually performed under local anesthesia as an outpatient procedure whereas conization procedures need general anesthesia and inpatient care. Regarding pregnancy outcomes, excisional treatment procedures, including cold-knife conization, laser conization, and LEEP, are associated with increased risk of adverse obstetric morbidity. In contrast, ablative procedures, including cryotherapy and laser ablation, are free of any of these untoward outcomes.[5,6] However, resected specimens from excisional procedures allow for precise histological diagnosis, including presence of unexpected microinvasive diseases, while ablative methods, by destroying cervical tissue, preclude this investigation and require additional pre-treatment biopsy. This ability to combine diagnosis with treatment in a single procedure remains an advantage of excisional treatments.

Women with high-grade CIN frequently undergo excisional treatments because, while more invasive, they are more definitive than ablative therapies. As such, there are few reports available regarding the efficacy of ablative treatments, such as laser ablation for high-grade CIN. Moreover, most studies comparing efficacy between treatments show both the rate of recurrence and residual disease, which is the failure rate; since these study populations often include a variety of CIN1 to CIN3 patients, and definitions for recurrence/residual disease depend on treatments, failure rates also vary markedly between studies. Both randomized and non-randomized studies demonstrate a failure rate of 5–30% for laser ablation and 5–16% for LEEP in a 6-month follow-up period;[7,8] however, in 2002, Dey *et al.* demonstrated that the cumulative risk of cytological abnormality reported as moderate dysplasia or worse is higher after laser ablation than LEEP.[9] A recent long-term follow-up study found cryotherapy was associated with the highest rate of recurrence compared with conization, LEEP, and laser ablation.[10] In total, the treatment efficacy against CIN has been still inconsistent comparing laser ablation against other excisional methods, such as conization and LEEP, and there is little information for the safety and efficacy of laser ablation for high-grade lesion.

In this study, we propose that laser ablation is a useful modality for the treatment of CIN in terms of obstetrics outcomes, even for high-grade lesions, if satisfactory colposcopy and consecutive cytology after treatment are available. In addition, we aimed to perform a descriptive investigation of the recurrence of high-grade CIN after laser ablation. Furthermore, the International Agency for Research on Cancer (IARC) announced in 2003 that among the over 100 HPV genotypes, 13 types (16, 18, 31, 33, 35, 39, 45, 51, 52, 56, 58, 59, 68, 73, and 82) should be considered carcinogenic, thus defined as 'high-risk types'.[11] Since then, HPV testing has been proposed as part of the follow-up of patients treated for high-grade CIN due to its very high sensitivity and negative predictive value for detecting residual/recurrent disease,[12] suggesting that it may be a good indicator of disease clearance. Indeed, a growing body of evidence has demonstrated that HPV testing together with cytology is useful in monitoring women treated for high-grade CIN.[12,13] To further clarify this in the setting of ablative therapy, we focused on the correlation between high-grade CIN recurrence rates and HPV genotype before and after laser ablation.

Methods

Patients

Following Japanese standard treatment protocols, in our study, those patients whose cervical biopsy demonstrated CIN3 (excluding CIS) and whose histology, cytology, and colposcopy were in concordance, were

treated with laser ablation between 2004 and 2010 at the Tokyo University Hospital. Patients were followed up with cytology and colposcopy 3 months after laser ablation, and those who showed residual disease were excluded from this study. Patients with negative cytology and normal colposcopic findings 3 months after treatment were included in this retrospective study. A total of 144 patients (mean age, 36.9 years; range, 25–71 years) met these criteria and were included in this retrospective study. Patients were followed up for at least 5 years with cytological and colposcopic evaluations conducted at intervals of 3–4 months. No residual lesion was confirmed by satisfactory colposcopic findings with negative cytology on the ecto-endocervix together. The recurrence of CIN3 was regarded as the primary end-point. Referring to the previous publications,[9,10] date of recurrence was defined as the mid-point between the date of the examination when abnormal cytology or histology (such as moderate-severe dysplasia, atypical squamous cells that cannot exclude HSIL [ASC-H], or high-grade squamous intraepithelial lesion [HSIL]) was first detected with satisfactory colposcopy, and the most recent preceding examination in which the colposcopic evaluations and smear (ecto-endocervix) were normal.

In total, 83 patients (median age, 36 years) were further examined for the efficacy of laser ablation by HPV genotypes, identified by polymerase chain reaction (PCR)-based HPV DNA testing before and after ablation, comparing the post-treatment persistent infection and recurrence-free survival (RFS) rates. HPV genotyping was performed in each patient. Regarding the natural history of CIN in Japan, a recent prospective cohort study by Matsumoto *et al.*[14] showed that the cumulative progression rate for CIN3 within 5 years was 20.5% for eight types of high-risk HPV (16, 18, 31, 33, 35, 45, 52, and 58), which was significantly higher than the 6.0% observed for five other high-risk types (39, 51, 56, 59, and 68), demonstrating that differences in progression exists even in the 13 HPV types defined by IARC as high-risk. In our study, therefore, we classified the study population according to this report and focused on the eight 'higher-risk' types. Informed consent was obtained in all cases. The median follow-up period was 17 months, with a minimum of at least 6 months. Recurrence was defined as emergence of CIN3 in complete responders.

PCR-based HPV DNA testing

DNA was extracted from cervical smear samples by using the QIAGEN DNeasy Blood & Tissue Kits. PCR-based HPV DNA testing was performed using the PGMY-CHUV assay. Briefly, standard PCR was conducted using the PGMY09/11 L1 consensus primer sets and HLA-dQ primer sets. Reverse blotting hybridization was subsequently performed as described previously.[15]

Laser ablation

Outpatient carbon dioxide laser procedures were carried out under colposcopic guidance, taking about 10 min, without anesthesia or premedication. Water in the tissue absorbs the laser energy, which destroys tissue by vaporization. To be effective, the lesion is typically ablated to a depth of 5 mm on the ectocervix and 8–9 mm around the endocervix. After ablation, the epithelium regenerates in 2–3 weeks. All cases were performed by gynecologic oncologists using CO2 laser, MEDILASER-30S (Model mel-30S, Mochida) with a power density of 8–12W in continuous mode.

Statistics

Date of recurrence was defined as the mid-point between the date of the examination when abnormal cytology was first detected and the most recent preceding examination in which the smear was normal. The log–rank test was used to assess differences in cumulative risk between study groups; tests of significance were carried out at the 5% two-sided level.

Results

We initially identified 144 patients with CIN3 who received laser ablation at Tokyo University Hospital between 2004 and 2010, and showed both negative cytology and normal colposcopic findings 3 months after treatment. Ten patients were excluded because of incomplete data. A total of 134 cases of CIN3 (median age, 37 years; range, 27–71 years, excluding CIS) were monitored every 3–4 months during the follow-up period (6–95 months; median, 38 months). Seven (5.2%) were censored at 1 year, 19 (14.2%) at 2 years, and 105 (78.4%) at 5 years after treatment. The recurrence of CIN3 was regarded as the primary end-point. All the patients were evaluated with satisfactory colposcopy and histological examination of transitional zone.

First, we investigated the efficacy of laser ablation against all CIN cases. During the follow-up period, recurrence was identified in 57 (42.5%) of the 134 patients, and the overall cumulative CIN3 recurrence rate in the first 12 months after treatment was 22.6%

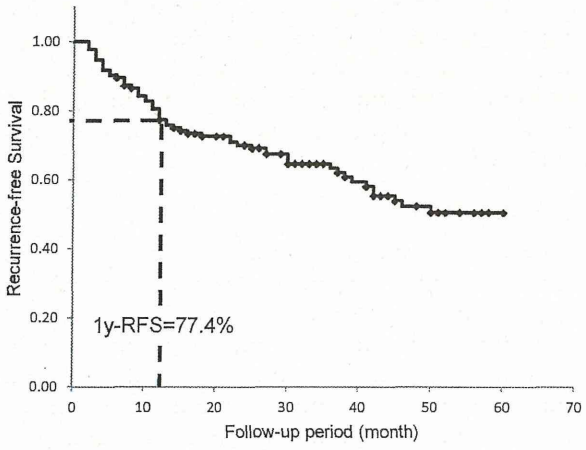

Figure 1 Overall cumulative recurrence rate after treatment. The overall cumulative recurrence rate of cervical intraepithelial neoplasia 3 in the first 12 months after treatment was 22.6%. RFS, recurrence-free survival.

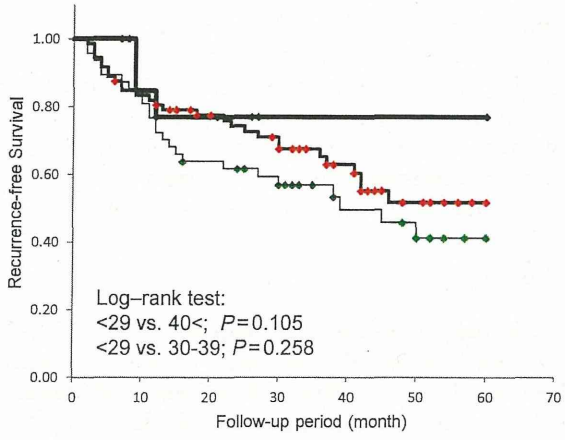

Figure 2 Recurrence rates compared by age. No significant elevated risk of recurrence was seen between younger age (<29) and older age (<29 vs >40; $P = 0.105$, <29 vs 30–39; $P = 0.258$, by log–rank test). ▬, <29; ▬, 30–39; —, 40<.

(Fig. 1). Figure 2 shows recurrence rates compared by age. It is worth noting that no significant elevated risk of recurrence was seen between younger age (<29) and older age (<29 vs >40, $P = 0.105$; <29 vs 30–39, $P = 0.258$, by log–rank test). Among recurrence cases, 27 patients underwent second laser ablation, nine patients underwent cervical conization, and one patient underwent total hysterectomy. Other patients were followed up with intensive cytological and colposcopic evaluations

Table 1 Distribution of HPV type before treatment

HPV type before treatment	Rate (%)
16	34
18	2
31	2
33	5
52	20
58	13
Others	24

The HPV genotypes of 83 patients were identified by polymerase chain reaction-based HPV DNA testing both before and after ablation. Seventy-six women were positive on HPV-DNA testing (91.6%). The distribution of HPV genotypes was classified according to the Matsumoto criteria of 8 'higher-risk' types. Two of the higher-risk types (35, 45) were not detected in this study. All cervical intraepithelial neoplasia 3 cases in this study had monoinfection. HPV, human papillomavirus.

with informed consent. The re-recurrence rate of CIN3 after second ablation was 11.1%.

Next, we evaluated the association between HPV genotype and efficacy of laser ablation, assessing whether HPV genotyping might predict failure after laser ablation. Of the 134 patients, we examined the HPV genotype of 83 patients, identified by PCR-based HPV DNA testing both before and after ablation. Single infection was observed in all CIN3 cases in this study, although there is a possibility that some patients might have multiple infections, especially in the CIN1-2 population. The median follow-up period was 17 months, with a minimum follow-up of 6 months. The median age of these 83 patients was 36 years; 76 women were positive on HPV-DNA testing (91.6%). The distribution of HPV genotypes, classified according to the Matsumoto criteria of eight 'higher-risk' types, before laser ablation is shown in Table 1.

Table 2 shows detection rates – that is, whether the same HPV type was detected before and after laser ablation, which can be interpreted as a good indicator of disease clearance. HPV was persistently detected after treatment more often in the higher-risk types, especially in type 16 and 18, than in other HPV types (16/18 vs 31/33/52/58 vs others; 66.6% vs 52.4% vs 25.0%; $P < 0.0001$ by Cochran–Armitage test).

In addition, we compared post-treatment RFS by HPV genotypes. As shown in Figure 3, we first compared RFS by pre-treatment HPV genotypes, that is, between those who were positive for the 8 higher-risk types and those positive for other HPV types before ablation; no statistically significant difference was seen between the two ($P = 0.77$ by log–rank test). We then

Table 2 Detection rate of HPV after treatment for each HPV type before treatment

HPV type before treatment	Detection of HPV after treatment†	
	Positive (%)	Negative (%)
16/18	66.6	33.3
31/33/52/58	52.4	47.6
Others	25.0	75.0

†Cochran–Armitage test $P < 0.0001$. Detection rates – i.e. whether the same HPV type was detected before and after laser ablation, which can be interpreted as a good indicator of disease clearance. HPV was persistently detected after treatment more often in the higher-risk types, especially in types 16 and 18, than in other HPV types (16/18 vs 31/33/52/58 vs others; 66.6% vs 52.4% vs 25.0%; $P < 0.0001$ by Cochran–Armitage test). HPV, human papillomavirus.

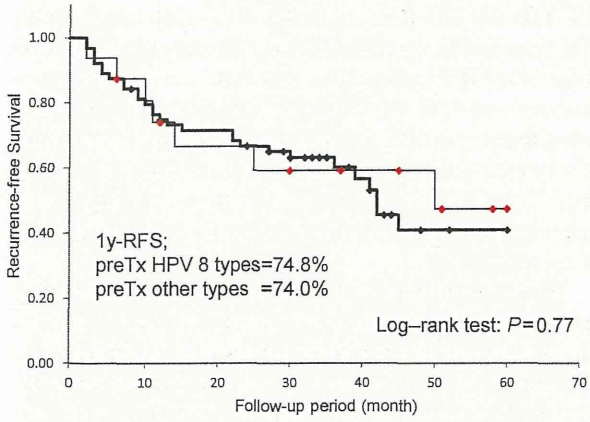

Figure 3 Recurrence-free survival (RFS) by pre-treatment human papillomavirus (HPV) genotype. We compared RFS between those who were positive for the 8 higher-risk types versus those positive for other HPV types prior to ablation; no significant difference between the two groups was identified. —, 8 types; —, Others.

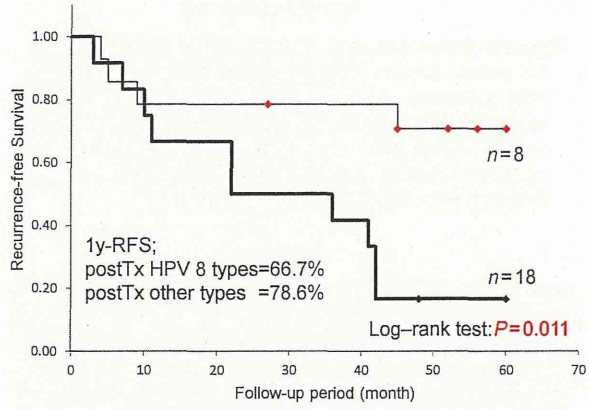

Figure 4 Recurrence-free survival (RFS) by post-treatment human papillomavirus (HPV) genotype. After ablation, 1-year RFS was 66.7% for those who were positive for the 8 higher-risk HPV types, which was significantly lower than the 78.6% observed in those positive for other HPV types. —, 8 types; —, Others.

compared RFS by post-treatment HPV genotypes. As shown in Figure 4, 1-year RFS was 66.7% for those who were positive for the 8 higher-risk types after ablation, which was significantly lower than the 78.6% observed in those positive for other HPV types ($P = 0.011$ by log–rank test). Furthermore, Figure 5 shows that the 1-year RFS for those positive for all high-risk 13 types of HPV after treatment was 61.1%, versus 100% in HPV-negative subjects ($P = 0.0013$ by log–rank test).

All these data suggest that the persistence of high-risk HPV genotypes, especially of the eight types, might play a key role in the development of recurrence.

Discussion

In 2011, a large Dutch multi-cohort study, one of the representative prospective studies on long-term efficacy of CIN treatment, reported on recurrence risk after treatment for CIN2/3.[16] According to that study, the recurrence risk of CIN was quite low after highly successful treatment followed by normal cytology or negative HPV testing. However, all participants were treated by excisional methods, such as cold-knife conization or LEEP, so the data did not present any information on the prognostic outcomes of conservative treatments, including laser ablation.

As mentioned, many studies have demonstrated that conservative methods, including cold-knife conization, LEEP, cryotherapy, and laser ablation, show similarly low morbidity and are equally successful at preventing invasive cervical cancer.[4,17,18] However, in 2009, Melnikow *et al.*[10] compared the long-term follow-up of 37 142 patients with CIN by treatment modality (cold-knife conization, LEEP, laser [conization and ablation